Science of the Total Environment 962 (2025) 178246

Contents lists available at ScienceDirect

Science of the Total Environment

journal homepage: www.elsevier.com/locate/scitotenv

Strong legacies of emerging trends in winter precipitation on the carbon-climate feedback from Arctic tundra

Elena Blanc-Betes [a,*,1], Jeffrey M. Welker [b,c], Nuria Gomez-Casanovas [d,e], Evan H. DeLucia [f], Josep Peñuelas [g,h], Eduardo Dias de Oliveira [i], Miquel A. Gonzalez-Meler [a]

[a] Department of Biological Sciences, University of Illinois at Chicago, Chicago, IL 60607, USA
[b] UArctic, Ecology and Genetics Research Unit, University of Oulu, Finland
[c] Department of Biological Sciences, University of Alaska, Anchorage, Anchorage, AK 99501, USA
[d] Texas A&M AgriLife Research Center, Vernon, Texas A&M University, TX 76384, USA
[e] Rangeland, Wildlife & Fisheries Management Department, Texas A&M University, TX 77843, USA
[f] Institute for Sustainability, Energy, and Environment, University of Illinois at Urbana-Champaign, Urbana, IL 61801, USA
[g] CSIC, Global Ecology Unit CREAF-CEAB-UAB, Cerdanyola del Vallès, 08193, Catalonia, Spain
[h] CREAF, Cerdanyola del Vallès, 08193, Catalonia, Spain
[i] The New Zealand Institute for Plant and Food Research Ltd, Havelock North 4157, New Zealand

HIGHLIGHTS

- Non-linear response of net C flux to snow: shallower and deeper snow depth reduce C losses from arctic tundra.
- Snow depth reshapes plant community, but CO_2 uptake is constrained by canopy structure.
- Reduced microbial respiration rather than enhanced plant productivity drives C sink with snow depth.
- Rhet limited by temperature and SWC rather accelerated by warming or thaw-induced C availability.
- CH_4 emissions amplify the GWP despite reduced C losses with deeper snow.

GRAPHICAL ABSTRACT

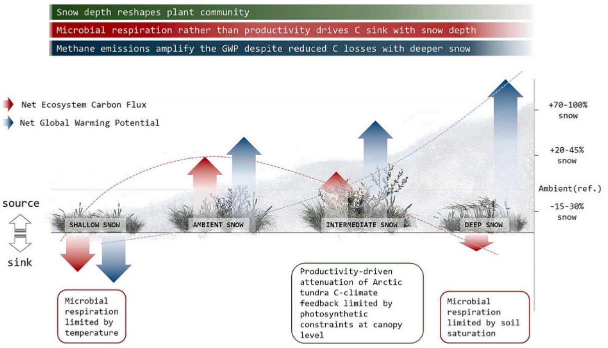

ARTICLE INFO

Editor: Roland Bol

Keywords:
Arctic tundra
Precipitation
Snow
Carbon-climate feedback
Climate change

ABSTRACT

Changes in winter precipitation accompanying emerging climate trends lead to a major carbon-climate feedback from Arctic tundra. However, the mechanisms driving the direction, magnitude, and form (CO_2 and CH_4) of C fluxes and derived climate forcing (i.e. GWP, global warming potential) from Arctic tundra under future precipitation scenarios remain unresolved. Here, we investigated the impacts of 18 years of shallow (SS, −15–30 %) and deeper (IS, +20–45 %; DS, +70–100 %) snow depth on ecosystem C fluxes and GWP in moist acidic tundra over the growing season. The response of Arctic tundra C fluxes to snow accumulation was markedly non-linear. Both shallow- and deeper- winter snow decreased Arctic tundra CO_2 emissions relative to ambient (AS), ultimately reducing ecosystem C losses over the growing season. Gross primary productivity (GPP) increased with

---

[*] Corresponding author at: Institute for Sustainability, Energy, and Environment, University of Illinois at Urbana-Champaign, Urbana, IL 61801, USA.
E-mail address: mblanc7@illinois.edu (E. Blanc-Betes).
[1] Present address.

https://doi.org/10.1016/j.scitotenv.2024.178246
Received 13 August 2024; Received in revised form 27 November 2024; Accepted 20 December 2024

Global warming potential
Carbon fluxes

moderate increases in snow depth and decreased with further snow accumulation closely following transitions in shrub abundance. Photosynthetic uptake, however, was tightly regulated by canopy structure and plant respiration (R_{aut}) to GPP ratio was highly conserved despite substantial transformations of plant community across snow treatments revealing a prominent role of heterotrophic respiration (R_{het}) in driving net ecosystem exchange. Consistently, ecosystem C gains responded to constraints on R_{het} by temperature limitation within colder soils at SS, and by snow- and thaw-induced increases in soil-water content (SWC) that promoted anaerobic decomposition and dampened the temperature sensitivity of R_{het} at IS and DS. Greater CH_4 emissions from wetter soils, however, increased the global warming potential (GWP) of Arctic tundra emissions at IS and DS despite decreases in C losses. Overall, our findings indicate the potential of Arctic tussock tundra to reduce C losses over the growing season but also to significantly contribute to the ecosystem GWP under emerging trends in winter precipitation.

1. Introduction

Permanently frozen soils (permafrost) contain over half of the terrestrial soil organic carbon (SOC) (Hugelius et al., 2014; Mishra et al., 2021). Arctic warming and changes in precipitation can increase the vulnerability of the permafrost carbon (C) pool, releasing ancient C into the atmosphere, thereby leading to a positive C-climate feedback (Crichton et al., 2016; Czimczik and Welker, 2010; Hicks Pries et al., 2016; Lupascu et al., 2014; Schuur et al., 2015, 2022). The magnitude, direction, and form (CO_2 and CH_4) of this climate feedback, however, remain uncertain (Burke et al., 2012a, 2012b; McGuire et al., 2016; Treat et al., 2024), largely due to a limited understanding of Arctic C responses to changes in winter precipitation (Koven et al., 2013; Rixen et al., 2022; Schädel et al., 2024; Schaefer et al., 2014).

Climate models consistently predict 25–50 % increase in Arctic precipitation by 2100, >50 % as winter snowfall (Bintanja and Selten, 2014; Khani et al., 2022; McCrystall et al., 2021; Zhang et al., 2013), but both increases beyond projections and decreases below the current average are expected (Callaghan et al., 2011; Khani et al., 2022; Kohler et al., 2006; Stocker et al., 2013; van Pelt et al., 2016) as reported in NOAA ARC (Mudryk et al., 2022). Snow depth and cover duration explain 50–100 % of the annual variability of soil temperature in Arctic systems (Gisnås et al., 2014; Lawrence and Slater, 2010). Deeper snow promotes soil warming directly through the insulating effect of snow over the snow-covered season, and indirectly over the growing season by increasing soil thermal conductivity and latent heat associated to increases in soil-water content (SWC) that derive from snow melt and the progressive thaw of the active layer (Liu et al., 2023; Morgner et al., 2010; Subin et al., 2013; Zhang, 2005; Zhang et al., 2013). Increases in snow accumulation account for up to 50 % of recent permafrost warming and thawing in Northern Alaska (Osterkamp, 2007; Stieglitz et al., 2003). The derived impacts on the soil thermal state and hydrology may result in cascading effects on soil C and N mineralization (Rixen et al., 2008; Schimel et al., 2004; Semenchuk et al., 2015) and plant community composition, phenology and productivity (Bosiö et al., 2014; Johansson et al., 2013; Kelsey et al., 2021; Leffler et al., 2016). The potential magnitude of the resulting C-climate feedback therefore implies an urgent need to resolve the complex interactions that govern the C cycle of terrestrial Arctic systems under future precipitation scenarios (Blanc-Betes et al., 2016; Carvalhais et al., 2014; Rixen et al., 2022).

Predictions of climate forcing from Arctic regions build upon a conceptual framework based on the net balance of two competing climate feedbacks (Koven et al., 2015a) (Fig. 1): i) a positive feedback from accelerated rates of decomposition through warming- and thaw-induced increases in SOC availability (i.e. turnover-driven acceleration of climate change) (Burke et al., 2018; Feng et al., 2020; Pedron et al., 2023; Schaefer et al., 2011; Xue et al., 2016); and ii) a negative feedback from increased plant productivity associated with enhanced nutrient mineralization and availability, typically linked to shrub expansion accompanying warming (i.e. productivity-driven attenuation of climate change) (Berner et al., 2020; DeMarco et al., 2014b; Kelsey et al., 2021; Mekonnen et al., 2018, 2021; Phoenix and Treharne, 2022; Salmon et al., 2016).

The mechanisms operating within this dual conceptualization of the Arctic system, however, remain unclear, especially in response to

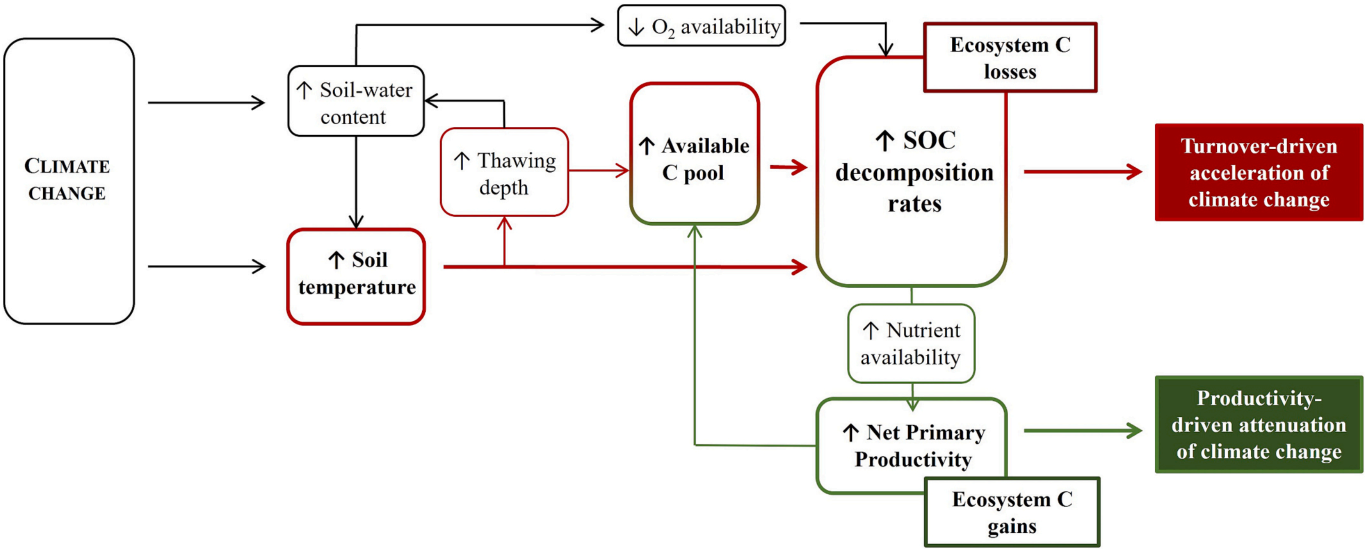

Fig. 1. Schematic illustrating the dual conceptualization of the C-climate feedback from terrestrial Arctic systems based on the net balance of a turnover-driven acceleration and a productivity-driven attenuation of climate change. In bold are the dominant mechanisms driving positive (red) and negative (green) C-climate feedback from terrestrial Arctic systems.

emerging changes in precipitation (Burke et al., 2017; Koven et al., 2015a). Experimental snow-depth manipulations, and soil warming and/or nutrient additions consistent with deeper snow have been shown to enhance, reduce and to have no effect on microbial activity, nutrient availability and uptake, and the leaf-level physiological responses of vegetation (Table S1). Discrepancies persist at the ecosystem level, the CO_2 sink or source strength of Arctic and subarctic tussock tundra displaying an equally wide array of responses (Table S1). Moreover, the response of Arctic tundra C fluxes to future climate responds to the integration processes that may differ in lag-times and sensitivities to disturbance and is hence unlikely to be permanent nor fixed. There is growing evidence of non-linearity in the response of Arctic C dynamics to warming and/or nutrient additions consistent with deeper winter snow, both over time and with level of disturbance (Arens et al., 2008; Mauritz et al., 2017; Schädel et al., 2018; Sharp et al., 2013; Weg et al., 2013). Predictions of long-term (i.e. decadal) climate feedbacks from Arctic regions under future precipitation scenarios from the extrapolation of short-term responses to a single-level disturbance are likely to result in inaccurate projections (Koven et al., 2015b; Luo et al., 2011). Multi-level, multi-year experimental studies are, therefore, critical to resolve regulatory processes and harmonize discrepancies, thereby contributing to the foundation of a sound understanding of the role of terrestrial Arctic systems in a changing climate.

Predictions of C-climate feedbacks from Arctic tundra are particularly sensitive to winter precipitation, as snow- and thaw-induced SWC, by limiting O_2 availability, may slow down SOC decomposition but stimulate CH_4 emissions (Blanc-Betes et al., 2016). Given the disproportionate global warming potential (GWP) of CH_4 (33 CO_2 equivalents) (Myhre et al., 2013), snow- and thaw-induced changes in SWC may introduce to up to 50 % divergence in model predictions of the resulting radiative forcing (Knoblauch et al., 2018; Lawrence et al., 2015; McGuire et al., 2012).

We investigated the long-term impact of changes in snow depth on the strength and regulation of the C sink and GWP of moist acidic tundra during the growing season. We combined measurements of plant-community structure and climatic variables with ecosystem, soil and heterotrophic CO_2 fluxes during the growing season after 18 years of snow depth increases and decreases. We estimated the impact of snow accumulation on the growing-season C budget (CO_2 and CH_4) and radiative forcing from Arctic tundra using concurrent measures of the ecosystem CH_4-C flux at each snow depth published elsewhere (Blanc-Betes et al., 2016). We hypothesized that a deeper and warmer active layer under deeper snow would accelerate SOC decomposition, but C losses would be partly or fully offset by higher GPP associated with shrub encroachment. Higher CH_4 emissions from increasingly wet soils with deeper winter snow, however, would increase the radiative forcing of C emissions from moist tussock tundra, which represents 40 % of the Alaskan tundra and 20 % of Arctic tundra (Forbes, 2015; Walker et al., 1994).

2. Material and methods

2.1. Site description

The research was conducted in moist acidic tussock tundra near Toolik Lake (68°38′, 149°38′W; 760 m) at the long-term US ITEX (International Tundra Experiment) in the northern foothills of the Brooks Range, Alaska (Walker et al., 1999). Annual air temperature averages −8 °C, with monthly mean summer temperatures of 7–12 °C. Mean annual precipitation from 1994 to 2023 was 293 mm (120–470 mm range), with approximately 50 % falling as snow (Deslippe and Simard, 2011; Environmental Data Center, Toolik Field Station, 2023). The study area remains covered in snow for about 265 days a year, with accumulations of 45–80 cm, and becomes snow-free by mid-June, marking the beginning of the growing season (Environmental Data Center, Toolik Field Station, 2023). The area is dominated by tussock-forming sedges (*Eriophorum vaginatum*) and mosses (*Sphagnum* spp., *Hylocomium splendens*), with scattered deciduous (*Betula nana*, *Salix pulchra*) and evergreen (*Cassiope tetragona*, *Rhododendron subarcticum*) shrubs (Wahren et al., 2005; Walker et al., 1994). The soil is a Ruptic-Histic Pergelic Cryaquept (Romanovsky et al., 2010). Soil is poorly drained, with a 10–15 cm organic horizon, and the active layer typically thaws to a maximum depth of 45–50 cm by the end of August.

2.2. Experimental design

An experimental snow fence (2.8 × 60 m) was installed in 1994 perpendicular to prevailing winter winds to create a snow drift extending 60 m downwind (Walker et al., 1999). We established five sampling plots in 2012 at each of four depths along the snow drift: 1) ambient snow (AS, annual maximum depth of 71 ± 6 cm), 2) shallow snow (SS, 15–30 % less snow than AS; annual maximum depth of <55 cm), 3) intermediate snow (IS, 20–45 % more snow than AS; annual maximum depth of 98 ± 7 cm), and 4) deep snow (DS, 70–100 % more snow than AS; annual maximum depth of 131 ± 16 cm) (Blanc-Betes et al., 2016; Jones et al., 1998; Pattison and Welker, 2014; Walker et al., 1999). IS represented an increase in snowfall estimated for the end of the current century (Bintanja and Selten, 2014). Plots 1–5 in treatments SS, IS and DS were established parallel to the fence from left to right. AS plots were perpendicular to the fence at equivalent distances from the fence as those of the treatments to integrate potential spatial heterogeneity that could occlude treatment responses. An analysis of variance found no significant within-treatment variation for any of the measurements reported and hence, plots were assumed to successfully integrate spatial variability within treatment.

Annual precipitation in 2012 was 287 mm, similar to the mean annual precipitation reported for the area since 1994, and the area became snow-free on 18 June, near the average snow-free date of 16 June (Environ. Data Center, TFS, 2023). The onset of the growing season was 3–5 days earlier in SS than AS and was delayed by 5–7 days in IS and 15–20 days in DS compared to AS.

Fluxes of ecosystem, soil and heterotrophic CO_2 and soil environmental variables (soil temperature, SWC and thaw depth) were measured biweekly from 30 May to 31 August 2012 (six sampling periods). Measurements were taken between 10:00 and 15:00 over three days. Net CH_4 fluxes were measured in parallel to CO_2 fluxes in all sampling plots and periods (for more detailed information, see Blanc-Betes et al., 2016). Measurements were randomized among plots and treatments to minimize confounding effects from daily variability. The plots were accessed from permanently installed boardwalks to minimize disturbance.

2.3. Microclimate measurements

Photosynthetically Active Radiation (PAR) and air temperature, were obtained hourly from a micrometerological station located 500 m from our site (Arctic LTER, Toolik Field Station; http://www.lternet.edu/sites/arc). PAR and air temperature were measured daily at the experimental site and agreed well with readings from the micrometeorological station ($r^2 = 98.6$; $P < 0.05$).

Soil temperature at 10-cm depth was measured at 0.5 h intervals during the growing season in each treatment using iButton temperature dataloggers to a precision of ±0.5 °C (Maxim Integrated Products, Sunnyvale, CA, USA) ($n = 3$). Handheld sensors were used to measure soil temperature (10-cm depth; OMEGA Engineering Inc., CT, USA) and 0–12 cm depth-integrated volumetric soil-water content (SWC) (HydroSense II, Campbell Scientific Inc., UT, USA). Thaw depth was measured using a metal rod calibrated in centimeter increments. Replicates of SWC and thaw depth ($n = 5$) were averaged values of 8 measurements (subreplicates) per plot and sampling time.

2.4. *Characterization of plant community*

Plant community at peak season (between late July for SS, AS and IS, and early August for DS) was characterized at each treatment ($n = 5$) with a 100-point 0.7 × 0.7 m grid following the point frame method (Walker, 1996). Unlike biomass sampling, this method was non-destructive, which is critical in this unique long-term experimental setup. Vegetation composition was expressed as percent coverage of the most common species comprising >80 % of the biomass of Alaskan tussock tundra, grouped by plant function (Walker, 1996). The aim was to determine whether changes in ecosystem fluxes responded to shifts in the dominant life forms. Spurious correlations were therefore intrinsic to any measure of dominance because an increase in dominance of one life form inevitably decreases the dominance of another.

2.5. *Measurement of ecosystem CO_2 flux*

Net ecosystem CO_2 exchange (NEE), the net balance between gross primary productivity (GPP) and ecosystem respiration (R_{eco}), were directly measured (NEE, R_{eco}) or estimated (GPP) at all treatments (n = 5) during the growing season. Midday NEE was measured as described by Shaver et al. (2007). Briefly, we used a Li-6400 (LI-COR Inc., Lincoln, USA) fitted to a custom-designed clear acrylic chamber (0.7 × 0.7 × 0.4 m) equipped with temperature and PAR sensors, and two internal fans. We constructed six-point light-response curves of NEE for each plot and sampling period corresponding to full ambient light, four levels of shade (ca. 15, 30, 50 and 70 %) and one dark-chamber measurement of R_{eco}. Chamber volume was corrected for plot-level microtopography by measuring the distance between the ground level and the base over a 100-point 0.7 × 0.7 m grid. Midday NEE and GPP fluxes were normalized to 600 μmol photons m^{-2} s^{-2} (NEE_{600} and GPP_{600}, respectively) using treatment- and period-specific model-fitted photosynthetic parameters (*Supp. Info.* A1).

2.6. *Effective leaf area index*

Effective leaf area index (i.e. effective LAI; reduction of true LAI based on the effect of nonrandom spatial distribution of foliage on LAI measurements) was estimated for each plot and period from the linear relationship between LAI and GPP_{600} described by (Street et al., 2007) for moist acidic tussock tundra near the area of study (slope = 6.7842; intercept = 0.732).

2.7. *Measurements of soil and heterotrophic respiration*

Soil CO_2 flux (R_{soil}) and its heterotrophic component (R_{het}) were measured at each treatment (n = 5) and sampling period using a Li-6400 infrared gas analyzer equipped with a 6400–09 soil chamber (LI-COR Inc., Lincoln, USA) fitted to previously installed soil PVC collars (10-cm diameter). The PVC collars were inserted to average depth of the Oe horizon (5–7 cm) for R_{soil} and to 50 cm for R_{het} installed before the first snow of the previous year (Voigt et al., 2016) following the root-exclusion method (Kuzyakov, 2006). Aboveground vegetation was removed from all collars upon installation, and vegetation regrowth, if any, was consistently clipped. Rates of R_{soil} were monitored until stabilized for two weeks before the start of the measurements, minimizing disturbance. We note that root exclusions for R_{het} are problematic (Hopkins et al., 2013) but large amount of SOC relative to root density are likely to minimize the impacts of the rhizosphere on R_{het} when compared to other ecosystems (Chen et al., 2013). Both R_{soil} and R_{het} were corrected for chamber volume accounting for depths of insertion of each collar. Replicates were averages of two pseudo-replicates of three cycles each per plot.

2.8. *Modeling seasonal gross primary productivity, ecosystem respiration and net ecosystem exchange*

Seasonal ecosystem CO_2 fluxes (GPP′, R'_{eco} and NEE′) at each treatment were estimated from gap-filling methods considering response functions to PAR and atmospheric temperature in each plot. Previous studies show that model parameterizations with midday values accurately predict daily CO_2 fluxes in Arctic systems (Sharp et al., 2013). We, therefore, used midday model-fitted parameters to estimate seasonal NEE using the Photosynthetic Irradiance-Response and Temperature-sensitive respiration model (PIRT) model (Williams et al., 2006). The PIRT model is a two-term algorithm that integrates ecosystem photosynthetic irradiance-response (i.e. GPP′) and develops the R_{eco} term as a function of the ecosystem respiration-temperature response (i.e. R'_{eco}) (*Supp. Info.* A2; Fig. S3). All model-fitted parameters are presented in Table 1.

To gauge confidence in our predictions, GPP′ was also estimated using an adaptation of the aggregated canopy photosynthesis model that uses parameterizations of the leaf-level photosynthesis-light response and light extinction through the canopy to integrate phenology (Ives et al., 2013; Sharp et al., 2013; Shaver et al., 2007) (*Supp. Info.*, A3; Fig. S4). Comparisons of predictions of GPP′ indicated strong agreement ($r^2 = 0.97$, $P < 0.0001$; slope = 0.93, intercept = 0.4) validating the photosynthetic irradiance-response term of the PIRT model for predicting GPP′, and the interpolation of period-specific parameterizations to integrate seasonality (Fig. S4). A regression of predicted against

Table 1

Results of the parameterization of the Photosynthetic Irradiance-Response and Temperature-sensitive respiration (PIRT) model. (a) Model parameters and statistics for each treatment developed from treatment-specific period averages. Model parameters are: light-saturated photosynthesis (A_{max}, μmol CO_2 m^{-2} s^{-1}), half-saturation constant (K_s, μmol photons m^{-2} s^{-1}), mean quantum efficiency (E_0, μmol CO_2 $μmol^{-1}$ PAR), leaf area index (LAI), basal ecosystem respiration (R_b, μmol CO_2 m^{-2} s^{-1} at 0 °C), relative increase in R_{eco} with air temperature (β, 1/°C) and the apparent temperature sensitivity of ecosystem respiration (Q_{10}) in each treatment. Values reported are seasonal means ± standard errors of the means. Different letters denote significant differences between snow treatments ($P < 0.05$). (b) Statistics of the fit when treatment-specific parameters are used to predict NEE in the entire data set. (c) Statistics of fit when treatment-specific parameters are used to predict NEE in a subset of data not included in the parameterization of the model.

	SS	AS	IS	DS
(a) PIRT model parameterization				
A_{max}	18.2 ± 1.1^a	22.0 ± 1.4^b	28.2 ± 1.1^c	20.4 ± 0.9^{ab}
Ks	711.3 ± 74.7^a	870.1 ± 80.3^{ab}	1019.4 ± 98.0^b	976.2 ± 77.8^{ab}
E_0	0.026 ± 0.003^a	0.025 ± 0.002^a	0.028 ± 0.002^a	0.021 ± 0.003^b
Effective LAI	1.08 ± 0.02^a	1.19 ± 0.02^b	1.42 ± 0.03^c	1.05 ± 0.02^d
R_b	1.57	1.72	2.17	0.31
β	0.078	0.080	0.075	0.177
Q_{10}	2.2	2.2	2.1	5.9
r^2	0.41	0.57	0.59	0.79
(b) Model evaluation				
Slope	0.954	0.968	0.972	0.965
Intercept	– 0.068	– 0.209	– 0.247	0.037
R^2	0.970	0.951	0.953	0.974
RMSE	0.960	1.298	1.342	0.877
n	180	180	180	120
(c) Model validation				
Slope	0.922	0.949	0.936	0.945
Intercept	0.166	– 0.452	– 0.407	0.336
R^2	0.974	0.919	0.936	0.968
RMSE	0.883	1.213	1.253	1.028
n	36	36	36	24

observed R_{eco} similarly indicated unbiased relationships for all treatments (Fig. S5).

Hourly GPP and R_{eco} were combined to estimate hourly NEE for each treatment, and the estimates were summed for calculating daily and seasonal GPP′, R'_{eco} and NEE′ for each treatment (*Supp. Info* A2; Fig. S6).

2.9. *Modeling soil, heterotrophic and autotrophic respiration*

Daily R_{soil} for each treatment was estimated by linearly interpolating R_{soil} between sampling periods (Gomez-Casanovas et al., 2013), and daily R_{het} was estimated from treatment-specific temperature-dependent functions following procedures in Lloyd and Taylor (1994) (*Supp. Info.*, A4). Model-fitted parameters are presented in Table 3.

Daily estimates of autotrophic respiration (R_{aut}; above- and belowground plant respiration) were calculated as the difference between R_{eco} and R_{het}, and daily estimates were summed to calculate seasonal R'_{aut} at each treatment (*Supp. Info.*, A4).

2.10. *Seasonal R'_{aut}-to-GPP′ ratios and net primary productivity*

The R_{aut} to GPP ratio was calculated for each treatment from seasonal estimates (i.e. R'_{aut}-to-GPP′). Seasonal net primary productivity (NPP′) was calculated for each treatment as the difference between seasonal estimates of GPP′ and R'_{aut}. R'_{aut} and GPP′ were measured independently, thus minimizing autocorrelation biases of calculated values as described in DeLucia et al. (2007) and Lasslop et al. (2010). R'_{aut}-to-GPP′ and NPP′, however, were used as an indication of change in response to treatment rather than a quantitative measure due to the inherent codependency between estimates of R_{aut} and GPP in this study.

2.11. *Seasonal ecosystem C budgets and GWP*

Seasonal ecosystem C budgets for each treatment were calculated from the sum of the net seasonal ecosystem CO_2 and CH_4 balance, accounting for the mass difference between CO_2 and CH_4 gas and expressed as gCO_2-C and gCH_4-C, respectively. The seasonal ecosystem CO_2 budget was inferred from NEE′ and seasonal net ecosystem CH_4 budget was calculated from linearly interpolated period- and site-specific mean fluxes from our parallel CO_2 flux measurements (Fig. 3 and Table 4 in (Blanc-Betes et al., 2016). The net seasonal ecosystem C flux for each treatment was expressed as CO_2 equivalents (CO_2e) by multiplying the seasonal CH_4 budget of each treatment by its 100-year GWP (33 CO_2e) (Myhre et al., 2013; Shindell et al., 2009) and adding its corresponding seasonal CO_2 budget for calculating GWP from ecosystem C fluxes during the growing season.

2.12. *Statistical analysis*

We used separate generalized linear mixed models for each dominant life form, with treatment as a fixed effect and plot as a random effect, for reporting changes in responses to treatments specific to the life form. Similar statistical methods have been used for analyzing the response of species coverage (%) to treatment (Bennie et al., 2018). We investigated the effect of the snow treatments on abiotic factors (air and soil temperature, volumetric SWC, and thaw depth), biotic variables (NEE_{600}, GPP_{600}, R_{eco}, and R_{het}), model-fitted parameters (A_{max} and K_s), and derived variables (effective LAI) using repeated-measures analyses of variance (repeated ANOVAs), with treatment (RS, Ambient, MS, and HS) and sampling period (1–6) as main effects, and plot within treatment ($n = 5$, except for R_{het} where $n = 3$) as a random effect. The effects of treatment on CO_2 fluxes within a period were examined by simple analysis of variance (ANOVA). Simple regression analyses were conducted to describe the responses of R_{eco}, R_{soil} and R_{het} responses to single environmental variables. Multiple regression analyses were performed to determine the combined effect of the abiotic variables on CO_2 fluxes. Normalized GPP_{600}, R_{eco}, and R_{het} were independently measured, thus minimizing spurious correlation and overestimation of regression coefficients derived from the calculation of autocorrelated variables as in (Lasslop et al., 2010). We subtracted self-correlation, however, by estimating the fraction attributed to shared variables (r^2_{SC}) (Gomez-Casanovas et al., 2012; Vickers et al., 2009) due to the inherent codependency between estimates of ecosystem CO_2 assimilation and respiration. All residuals were checked for normality and homogeneity of variances to ensure that the assumptions of the ANOVAs and regressions were met, and the statistical significance was determined at $P < 0.05$. Error term for the seasonal budgets of ecosystem CO_2 and CH_4 fluxes, and soil and heterotrophic CO_2 fluxes were propagated using daily variance as the main parameter representing the uncertainty associated with spatial heterogeneity within treatment (Davidson et al., 2008). All statistical tests were conducted with Statgraphics Centurion XVI (Statistical Graphics Corporation).

3. Results

3.1. *Environmental parameters*

Deeper winter snow led to warmer soil temperatures over the growing season despite an early season short-lived cooling effect associated with delayed snowmelt (Fig. S1a). Differences among treatments increased as the season progressed ($P < 0.05$). SS averaged colder soils than AS over the growing season (1.8 ± 0.07 and 2.4 ± 0.1 °C, respectively; $P < 0.05$), and seasonal soil temperature increased with deeper snow in IS and DS (3.5 ± 0.08 and 4.1 ± 0.04 °C, respectively; $P < 0.05$).

Volumetric SWC increased with snow depth and during the growing season in all treatments except for DS where the soil was saturated throughout the season (Fig. S1b). Soils were drier in SS (0.63 ± cm^3 cm^{-3}; $P < 0.05$) and wetter in IS and DS (0.88 ± 0.02 and 0.96 ± 0.03 cm^3 cm^{-3}, respectively; $P < 0.05$) than in AS (0.71 ± 0.03 cm^3 cm^{-3}).

Thaw depth increased with snow depth, and differences among treatments intensified as the season progressed ($P < 0.05$) (Fig. S1c). Maximum thaw depth was similar in SS and AS (49.3 ± 1.1 and 51.1 ± 1.6 cm, respectively; $P > 0.1$), and increased in IS and DS (56.7 ± 1.4 and 65.8 ± 2.3 cm, respectively; $P < 0.05$).

Seasonal atmospheric temperature averaged 12.1 °C, with the highest monthly mean occurring in July (14.4 °C) (Fig. S3a). PAR was highest in June and decreased thereafter registering <600 μmol photon m^{-2} s^{-1} during 90 % of August (Fig. S3a).

3.2. *Characterization of vegetation cover*

The relative abundance of shrubs increased with moderate increases in snow depth from SS (22.5 ± 3.3 %) to AS (27.4 ± 3.1 %) to IS (32.0 ± 3.6 %) but decreased with further snow accumulation in DS (9.2 ± 1.6 %) (Fig. 2). Eighteen years of shallower snow-depth reduced the presence of deciduous shrubs by 56 ± 3 %, while increased the presence of evergreen by 10 ± 4 % in SS. In IS, deciduous shrubs increased by 87 ± 4 % while evergreen shrubs decreased by 36 ± 3 % relative to AS (Fig. 2). In contrast, both deciduous and evergreen shrubs decreased in DS by 25 ± 3 % and 97 ± 2 % compared to AS, respectively (Fig. 2). The relative abundance of graminoids decreased from 17.9 ± 2.7 % in AS to 15.5 ± 3.4 % in SS but increased in IS and DS to 21.7 ± 2.2 % and 27.6 ± 3.4 %, respectively. The relative abundance of mosses was similar in SS, AS and IS (11.4–12.7 %) but was higher in DS (54.2 ± 3.6 %).

3.3. *Ecosystem, soil and heterotrophic CO_2 fluxes*

Mean GPP_{600} increased in IS and decreased in DS relative to AS and SS (Fig. 3a). Mean GPP_{600} was similar in SS and AS despite lower A_{max} due to smaller Ks (Figs. 3a and S2, Tables 1 and S2). GPP_{600} was consistently higher in IS than in AS during the growing season despite increased Ks due to a higher A_{max} (Figs. 3a and S2, Tables 1 and S2). However, further snow accumulation reduced GPP_{600} due to lower A_{max}

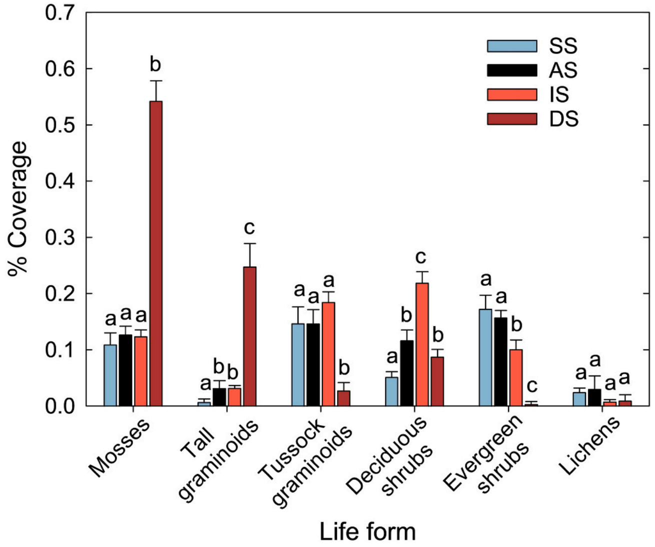

Fig. 2. Percent coverage of the main life forms for shallow snow (SS), ambient (AS), intermediate snow (IS) and deep snow (DS). Mosses include *Spagnum* sp. and *Hylocomium splendens*, tall graminoids are dominated by *Carex bigelowii*, tussock-forming graminoids refer to *Eriophorum vaginatum*, deciduous shrubs are dominated by *Betula nana*, *Salix pulchra* and *Vaccinum ulginosum*, evergreen shrubs include *Vaccinum vitis-ideae*, *Ledum decumbens* and *Cassiope tetragona* and lichens are dominated by *Peltigera* sp. and *Cladina* sp. Values are mean percent coverages ($n = 5$). Different letters for the same life form indicate significant differences among the treatments (ANOVA, $p < 0.05$). Error bars correspond to standard errors of the means.

and higher Ks in DS compared to AS (Figs. 3a and S2, Tables 1 and S2). Co-variation of A_{max} and Ks across treatments yielded relatively constant E_0, although E_0 increased slightly from SS and AS to IS ($P < 0.1$) and decreased in DS to below AS values ($P < 0.05$) (Tables 1 and S2).

Deeper snow increased R_{eco} from SS to AS to IS, but further snow accumulation in DS decreased R_{eco} (Fig. 3b, Table S2). The seasonal variation of R_{eco} was mainly driven by air temperature ($r^2 = 0.51$, $P < 0.05$) but differences in R_{eco} among treatments were mostly explained by changes in GPP_{600} (Table 2). After correction for self-correlation, the correlation between R_{eco} and GPP_{600} varied among treatments, increasing from SS to AS to IS, but decreasing in DS (Table 2). NEE_{600} thus illustrated a source-sink relationship with snow depth (Fig. 3c).

Rates of R_{soil} increased from SS to AS to IS but decreased in DS relative to AS (Fig. 4a, Table S2). Rates of R_{soil} were positively correlated with GPP_{600}, but correlation coefficients varied among treatments, increasing from SS to AS to IS, but decreasing in DS after adjusting for self-correlation (Table 2).

Rates of R_{het} were consistently lower in SS and higher in IS than in AS (Fig. 4b; Table S2). R_{het}, however, was similar in DS and AS (Fig. 4b, Table S2). Soil temperature and SWC explained variations in R_{het} (Fig. 5; Table 3). The apparent seasonal Q_{10} of R_{het} decreased slightly from SS to AS to IS, and substantially in DS (Table 3). Basal R_{het} (R_0; R_{het} at 0 °C) was unaffected by snow treatment (Table 3). R_{het} increased with SWC peaking at 0.65–0.77 $cm^3\ cm^{-3}$ but decreased with further increases in SWC (Fig. 5). The relative weights of soil temperature and SWC in explaining variations in R_{het} differed among treatments, with soil temperature losing leverage as SWC gained control with deeper snow (Table 3).

3.4. Effective leaf area index

Snow treatment altered effective LAI (Tables 1 and S2). Estimates of effective LAI increased from SS to AS to IS but decreased in DS to below AS (Tables 1 and S2).

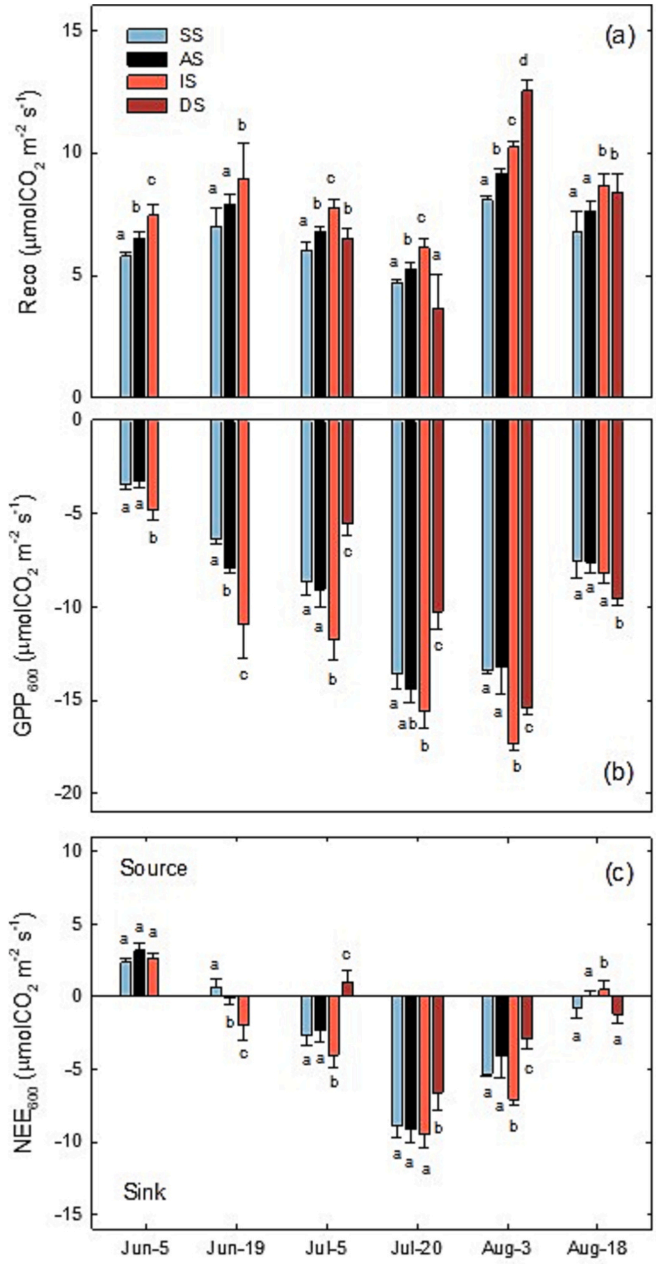

Fig. 3. Seasonal variation of the rates of (a) ecosystem respiration (R_{eco}) (b) gross primary productivity normalized to 600 μmol photons $m^{-2}\ s^{-1}$ (GPP_{600}), and (c) normalized net ecosystem exchange (NEE_{600}) for shallow snow (SS), ambient (AS), intermediate snow (IS) and deep snow (DS) (μmol $CO_2\ m^{-2}\ s^{-1}$). Normalized ecosystem CO_2 fluxes are reported from the atmospheric perspective, in which negative values indicate a CO_2 sink, and positive values indicate a CO_2 source. Different letters within the same sampling period indicate significant differences among the treatments (ANOVA; $p < 0.05$, n = 5). Error bars correspond to standard errors of the means.

3.5. Seasonal CO_2-C budgets

Both cumulative GPP′ and R'_{eco} were lower in SS and higher in IS than AS. Further snow accumulation in DS, however, decreased both GPP′ and R'_{eco} compared to AS (Fig. 6a and b). During the growing season, Arctic tundra was a net CO_2 source in AS and a net CO_2 sink in SS (Figs. 6c and 7a). Deeper snow reduced CO_2 losses in IS compared to AS and switched the system into a weak CO_2 sink in DS (Figs. 6c and 7a, Table S2). AS transitioned from a CO_2 source to a CO_2 sink by mid-July (Fig. 6c). The transition was anticipated by 5 and 12 days in SS and IS

Table 2
Results from the simple regression analyses. Evaluation of the relationship between GPP_{600} (ln-transformed) and ecosystem and soil respiration (μmol m^{-2} s^{-1}). Coefficients of determination considering raw regression (r^2), estimated self-correlation between co-dependent variables (r^2_{sc}) and estimated real correlations between variables subtracting inherent co-dependency ($\hat{r}^2$) are reported.

Dependent variable		r^2	r^2_{sc}	$\hat{r}^2$	F	P
R_{eco}	All treatments	0.16	0.12	0.04	18.8	<0.0001
	SS	0.42	0.08	0.34	15.9	0.0006
	AS	0.50	0.08	0.42	23.4	0.0001
	IS	0.74	0.08	0.66	64.6	<0.0001
	DS	0.48	0.26	0.23	12.2	0.004
R_{soil}	All treatments	0.29	0.01	0.28	40.4	<0.0001
	SS	0.32	0.00	0.32	12.8	0.0013
	AS	0.51	0.01	0.50	29.2	<0.0001
	IS	0.66	0.01	0.65	53.7	<0.0001
	DS	0.28	0.01	0.27	6.5	0.0207

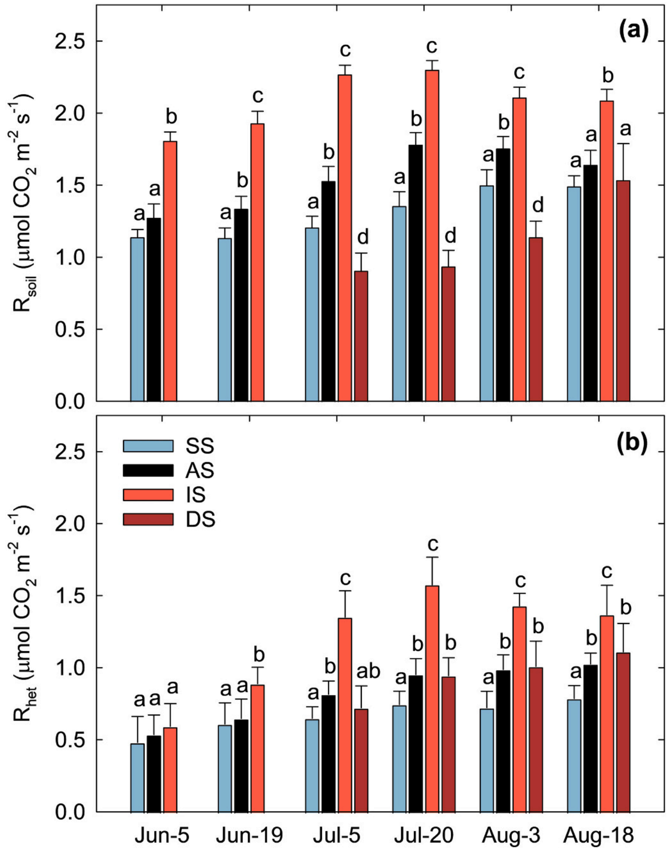

Fig. 4. Seasonal variation of the rates of (a) soil respiration (R_{soil}) and (b) heterotrophic respiration (R_{het}) (μmol CO_2 m^{-2} s^{-1}) for shallow snow (SS), ambient (AS), intermediate snow (IS) and deep snow (DS). Different letters within the same sampling period indicate significant differences among the treatments (ANOVA; $p < 0.05$, n = 5). Error bars correspond to standard errors of the means.

and delayed by 19 days in DS relative to AS (Fig. 6c). Both AS and IS became a net CO_2 source by late August, whereas SS and DS remained net CO_2 sinks until the first snow (Fig. 6c).

The contribution of R'_{het} to R'_{eco} was 15 ± 1.5 % in SS, 20 ± 1.2 % in AS, 21 ± 1.0 % in IS and 26 ± 1.7 % in DS. The contribution of R'_{het} to R'_{soil} was 50.7 ± 4.5 % in SS, 51.2 ± 3.2 % in AS, 58.2 ± 3.0 % in IS and 87.3 ± 7.9 % in DS.

The R'_{aut}-to-GPP′ ratio was similar between SS, AS and IS ($P > 0.05$), and decreased in DS ($P < 0.05$). R'_{aut}-to-GPP′ ratios were 0.64 ± 0.06 for SS, 0.68 ± 0.06 for AS, 0.61 ± 0.05 for IS, and 0.58 ± 0.05 for DS. NPP′ increased at SS and DS and was significantly higher at IS ($P < 0.05$) compared to AS (Fig. 8). Cumulative NPP′ during the growing season was 71.7 ± 8.8 gCO_2-C m^{-2} at SS, 65.0 ± 6.3 gCO_2-C m^{-2} at AS, 91.9 ± 6.9 gCO_2-C m^{-2} at IS, and 71.2 ± 6.2 gCO_2-C m^{-2} at DS.

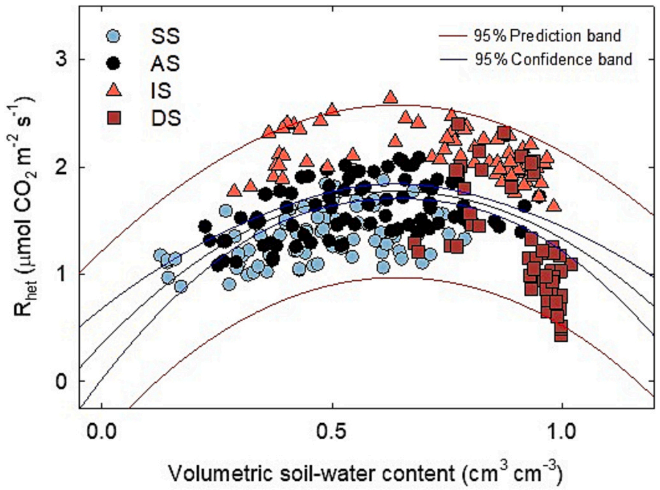

Fig. 5. Results from the simple regression analysis. Evaluation of the relationship between volumetric soil-water content (SWC, cm^3 cm^{-3}) and heterotrophic respiration (R_{het}, μmol CO_2 m^{-2} s^{-1}) during the growing season for shallow snow (SS), ambient (AS), intermediate snow (IS) and deep snow (DS).

Table 3
Results from the simple regression analyses. Evaluation of the relationships between heterotrophic respiration (R_{het}, μmol m^{-2} s^{-1}) and (a) volumetric soil-water content, (b) soil temperature and (c) thaw depth. Coefficients of determination (r^2) and statistics across treatments and for each individual treatment are reported. (b) shows basal respiration (R_0, μmol CO_2 m^{-2} s^{-1} at 0 °C), relative increase in R_{het} with air temperature (φ, 1/°C) and the apparent temperature sensitivity of R_{het} (Q_{10}) for each treatment. Different letters denote significant differences between snow treatments ($P < 0.05$).

	All treatments	SS	AS	IS	DS
(a) Volumetric soil-water content (cm^3 cm^{-3}). Best fit: polynomial					
r^2	0.31	0.48	0.50	0.64	0.88
RMSE	0.078	0.141	0.045	0.143	0.047
F	13.4	5.9	4.5	11.8	41.2
P	<0.0001	0.0147	0.0441	0.0012	<0.0001
(b) Soil temperature (°C). Best fit: exponential					
R_0	0.602	0.429^{a}	0.478^{a}	0.494^{a}	0.490^{a}
φ	0.142	0.237^{a}	0.220^{a}	0.247^{a}	0.158^{b}
Q_{10}	4.1 ± 1.5	10.7 ± 1.3^{a}	9.0 ± 1.2^{a}	8.6 ± 1.3^{a}	4.8 ± 1.3^{b}
r^2	0.56	0.87	0.85	0.81	0.77
RMSE	0.142	0.074	0.053	0.070	0.076
F	77.1	89.7	100.2	80.2	41.2
P	<0.0001	<0.0001	<0.0001	<0.0001	<0.0001
(c) Thaw depth (cm). Best fit: linear					
r^2	0.00	0.14	0.15	0.01	0.07
RMSE	0.223	0.210	0.131	0.233	0.159
F	0.2	1.3	1.4	0.1	1.0
P	0.6391	0.2835	0.2645	0.7928	0.3466

3.6. Seasonal ecosystem C budget and global warming potential

The Arctic tundra was a net source of C and GWP in AS when ecosystem CH_4 fluxes were incorporated into the seasonal C budget (Fig. 7). SS converted the tundra into a net sink of both C and GWP (Fig. 7). IS reduced net C losses by 30 ± 4 % but did not affect the GWP relative to AS when accounting for the radiative forcing of a 20-fold increase in the strength of the CH_4 source (Fig. 7). Further snow

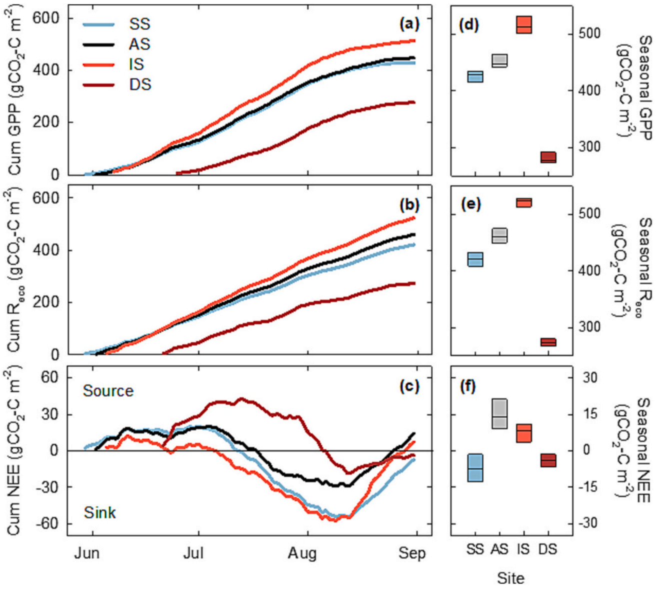

Fig. 6. Estimates of cumulative fluxes (a, b and c) and seasonal budgets (d, e and f) of ecosystem CO_2 fluxes including gross primary productivity (GPP') (a and d), ecosystem respiration (R'_{eco}) (b and e) and net ecosystem exchange (NEE') (c and f) expressed in gCO_2-C m^{-2} for shallow snow (SS), ambient (AS), intermediate snow (IS) and deep snow (DS) during the growing season. The box plots indicate model uncertainty for each CO_2-C seasonal budget (GPP', R'_{eco} and NEE') and site (SS, AS, IS and DS).

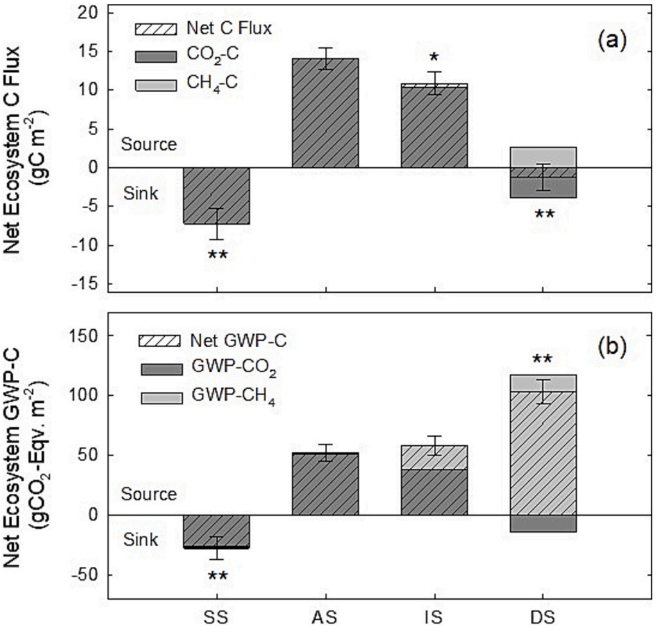

Fig. 7. Seasonal estimates of (a) net ecosystem C fluxes (gC m^{-2}) and (b) net C global-warming potential (GWP-C, patterned; gCO_2 equivalents m^{-2}) derived from the budgets of net ecosystem CO_2 (solid dark gray) and CH_4 (solid light gray) for shallow snow (SS), ambient (AS), intermediate snow (IS) and deep snow (DS). Error bars correspond to standard errors of the means. Asterisks indicate significant differences between a treatment and AS at $P < 0.1$ (*) and $P < 0.05$ (**). Error terms and statistical significance for individual contributions from CO_2 and CH_4 fluxes to net C and GWP budgets are displayed in Figs. S10 and S11 of Supp. Info.

accumulation in DS switched the system into a small C sink but increased the strength of the GWP source by 130 ± 16 % due to a 150-fold increase in the CH_4 source strength compared to AS (Fig. 7).

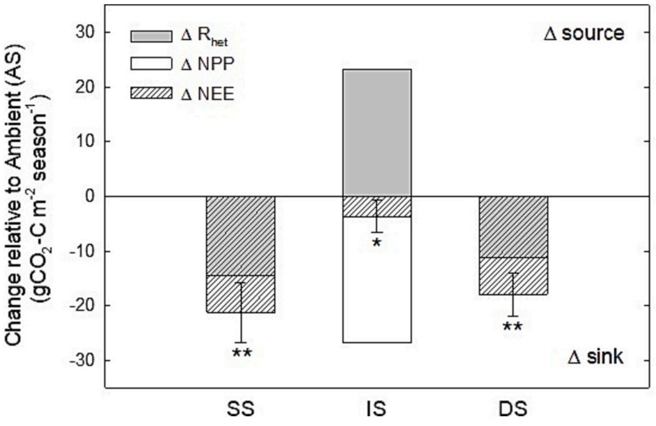

Fig. 8. Changes in the contribution of seasonal net primary productivity ($\Delta NPP'$) and heterotrophic respiration ($\Delta R'_{het}$) during the growing season to changes in net ecosystem exchange ($\Delta NEE'$) for shallow snow (SS), intermediate snow (IS) and deep snow (DS) relative to ambient (AS). Negative values indicate increases in the seasonal CO_2 sink in response to the treatments. $\Delta R'_{het}$ was significant for all treatments ($P < 0.05$), whereas $\Delta NPP'$ was significant for IS only ($P < 0.05$) ($P > 0.1$ for SS and $P = 0.1$ for DS). Error bars correspond to standard errors of the means of seasonal NEE. Asterisks indicate significant differences between a treatment and AS at $P < 0.1$ (*) and $P < 0.05$ (**). Error terms and statistical significance for individual contributions from R'_{het} and NPP' are displayed in Fig. S12 of Supp. Info.

4. Discussion

Carbon fluxes from Arctic tundra under Ambient conditions were similar in magnitude to those reported across the Alaskan Arctic tundra over the last decades, indicating that our study site was representative of moist acidic tundra in the region (Biasi et al., 2014; Grogan and Chapin III, 2000, 1999; Jones et al., 1998; Kwon et al., 2006; Leffler et al., 2016; Welker et al., 2000). Nearly two decades of both increases and decreases in winter snow depth reduced net C losses from moist acidic tundra during the growing season revealing a markedly non-linear response of NEE to snow accumulation. Seasonal CH_4 emissions, however, increased exponentially with deeper snow (Blanc-Betes et al., 2016), amplifying the GWP of the tundra with deeper snow despite decreases in C losses. Our results further revealed key regulatory pathways that depart from the turnover-driven acceleration vs productivity-driven mitigation framework (Fig. 1) in important ways, which we discuss in detail below: 1) GPP increased with moderate increases in snow depth and decreased with further snow accumulation in close correspondence with changes in shrub abundance, but enhanced photosynthetic CO_2 uptake typically linked to shrub expansion was largely constrained by canopy structure (i.e. three-dimensional arrangement of plant canopy); 2) a relatively conserved R_{aut}-to-GPP ratio across treatments limited the response of NPP, and revealed a prominent role of R_{het} in driving responses of the C sink or source strength and GWP of Arctic tundra to snow accumulation (Fig. 8); and 3) variations in R_{het} responded mostly to temperature constraints under shallow snow, and to SWC rather than to warming- and thaw-induced increases in C availability and decomposability with deeper snow.

4.1. Snow depth exerted a strong control on the productivity of Arctic tundra through impacts on plant community and canopy structure

Moderate increases in snow depth (from SS to AS to IS) increased the ecosystem photosynthetic activity accompanying the relative abundance of deciduous shrubs, which increased to the detriment of evergreens and sedges. This is consistent with changes in plant community structure observed at our experimental sites after 8 years of 1–3 fold snow depth increases (Wahren et al., 2005), and supports observations of recent shrub expansion in Arctic tundra accompanying climate warming (Callaghan et al., 2022; Elmendorf et al., 2012a, 2012b; Mekonnen et al., 2021; Tape et al., 2006, 2012; Walker et al., 2006). However, further snow accumulation (DS) drastically reduced GPP following the replacement of both deciduous and evergreen shrubs with tall sedges and mosses (Fig. 2, Fig. 6a). Similar transitions towards wet sedge tundra have been reported associated with progressive permafrost degradation (Myers-Smith et al., 2020).

Observed responses of ecosystem productivity to snow accumulation contrast with previous measurements of leaf-level photosynthesis across our experimental site, which declined with shallower snow (Pattison and Welker, 2014) and were not affected by increases in snow depth (Leffler et al., 2016). This apparent discrepancy suggests that changes in the maximum photosynthetic capacity (A_{max}) and GPP resulted from changes in effective LAI rather than in leaf-level physiology (Jespersen et al., 2023; Sharp et al., 2013; Starr et al., 2008; Street et al., 2007). Consistently, effective LAI closely followed changes in A_{max} (Fig. S2, Tables 1 and S2). This agrees with greater LAI, branching and secondary growth of deciduous shrubs in response to experimental warming and fertilization (Bret-Harte et al., 2002, 2001; Mekonnen et al., 2021; Shaver et al., 2001).

The denser canopy of a deciduous shrub-dominated overstory however, comes to the detriment of shaded understory vegetation (Bret-Harte et al., 2001; Miller and Smith, 2012), leading to higher A_{max}, but increasing light requirements (Ks, half-saturation light) and exerting a strong control on photosynthetic activity through canopy structure (Table 1; Fig. S2) (Sweet et al., 2015). Consistently, Ks and A_{max} increased proportionally yielding relatively conserved A_{max}-to-Ks values (E_0), and hence limiting the response of GPP to moderate changes in snow-depth (Table 1). Similarly, photosynthetic controls at the canopy level led seasonal development and mediated certain decoupling between seasonal GPP and the length of the snow-free period, challenging the tight correlation suggested by previous studies (Groendahl et al., 2007; Lund et al., 2010; Wipf and Rixen, 2010) (Figs. 3a, 6a and S2; Table 1).

4.2. *Heterotrophic respiration dominated the response of the Arctic tundra C budget to changes in winter snow with limited contribution from net primary productivity*

Changes in GPP with snow treatment were largely compensated by changes in R_{eco}, which integrates C losses from both plant R_{aut} and R_{het}. Consistently, GPP_{600} and R_{eco} were positively correlated in all treatments suggesting important contributions from R_{aut} to R_{eco} (r^2_{SC}; Table 2) (Gomez-Casanovas et al., 2012; La Puma et al., 2007). GPP_{600} explained an increasing portion of the R_{eco} variability with moderate increases in snow-depth but lose leverage with further snow accumulation, indicating greater uncoupling between ecosystem productivity and respiration with both shallow and deep snow accumulation (Table 2). This photosynthesis-to-respiration uncoupling may be traced to differences in the fraction of GPP lost through R_{aut} and to differences in R_{het}.

The proportion of GPP lost to R_{aut} (R_{aut}-to-GPP ratio) was highly conserved from shallow to ambient to intermediate snow depths (SS to AS to IS, respectively), suggesting little impact of moderate increases in snow depth on the plant carbon use efficiency (CUE; proportion of GPP allocated to biomass) despite higher GPP and shrub abundance. However, further snow accumulation decreased the R_{aut}-to-GPP ratio at DS despite significantly lower GPP, presumably due to the greater CUE of mosses (Bradford and Crowther, 2013; Street et al., 2013). Relatively conserved R_{aut}-to-GPP ratios among treatments indicates that variations in NEE were largely attributable to the direct impact of winter snow accumulation on R_{het}. Consistently, at SS and DS, 65–70 % of observed ecosystem C gains was attributable to decreases in R_{het}. Moreover, while NPP dominated changes in NEE at IS (responsible of 54 % of the observed change), C gains were partly offset by warming-driven increases in R_{het} limiting changes in the C sink strength despite evidence of substantial shrub expansion (Fig. 8).

4.3. *The dominant effect of R_{het} on the C sink strength responded to temperature and SWC constraints rather than warming and thaw-induced changes in C quality and availability*

R_{het} exhibited apparent seasonal Q_{10} values of ~10 at SS, AS and IS, and ~5 at DS (Table 3). These results agree with those reported for tussock and wet-sedge Arctic tundra soils (9.4 and 4.6, respectively) (Mikan et al., 2002) and are consistent with observed shifts in plant community across treatments (Fig. 2). Values of Q_{10} above 2.5 however, suggest that other variables such as SWC and substrate supply may covary with soil temperature to explain changes in R_{het} (Davidson et al., 2006; Davidson and Janssens, 2006; Hursh et al., 2017; Mishra et al., 2021). The high Q_{10} of Arctic soils has been suggested to largely reflect the temperature sensitivity of relatively labile SOC (Gentsch et al., 2018; Mikan et al., 2002). Recent studies propose that litter quantity (Myers-Smith and Hik, 2013) and quality (DeMarco et al., 2014a) are more important than environmental variables in determining decomposition rates. However, similar R_0 (i.e. R_{het} at 0 °C) suggests comparable substrate utilization across snow treatments despite the greater decomposability of graminoid-derived litter than that of deciduous shrubs (Fig. 2; Table 3) (Hobbie, 1996; Mack et al., 2004; Mikan et al., 2002). Similarly, R_0 did not respond to deeper and warmer active layer questioning arguments of thaw-induced shifts in substrate utilization (Biasi et al., 2005; Ren et al., 2020; Uhlířová et al., 2007). This is further supported by the negligible effect of thaw depth on R_{het} (Table 3). These results suggest that microbial activity and function responded to soil temperature and SWC constraints rather than plant-derived or thaw-induced changes in C availability and decomposability.

Volumetric SWC explained an increasing fraction of R_{het} variability from SS to AS to IS and became the main driver at DS (Table 3), where near water-saturation conditions limited aerobic decomposition within anoxic soils (Fig. 5) (Blanc-Betes et al., 2016). Consistently, Q_{10} decreased at DS, explaining similar R_{het} rates than AS despite substantial increases in soil temperature (Fig. 4; Table 3). This is consistent with the negative relationship between water table position and ecosystem Q_{10} reported from subarctic and Arctic regions (Huemmrich et al., 2010; McConnell et al., 2013).

4.4. *CH_4 fluxes increased the GWP Arctic tundra emissions with deeper snow despite lower C losses*

Snow- and thaw- induced increases in SWC limited R_{het} contributing to the C sink strength of Arctic tundra with snow additions (Fig. 7a). This additional C sink, however, came at the cost of substantial positive feedback on climate (GWP), as near water-saturated conditions significantly increased CH_4 emissions from Arctic tundra under deeper snow (Fig. 7b) (Blanc-Betes et al., 2016). These results agree with model predictions of climate forcing feedbacks from Arctic regions considering the prognostic dynamics of incomplete permafrost degradation (Grant, 2015; Knoblauch et al., 2018), but contrast with model projections addressing scenarios of extensive losses of permafrost area by the end of the century (Burke et al., 2012a, 2012b; Koven et al., 2015b; Schaefer et al., 2011).

4.5. *Implications*

Nearly two decades of changes in snow-depth led to legacies onto the functioning and regulation of C dynamics over the growing season and reshaped the plant community of moist acidic tundra. Increases in snow-depth consistent with observations (Pedersen et al., 2021; Stuefer et al., 2020) and projections of winter precipitation (Bintanja and Selten, 2014) in Arctic systems facilitated shrub encroachment, increases in leaf area and accelerated green-up rates in line with ecological definitions of Arctic greening (Callaghan et al., 2022). Further snow accumulation, however, drastically reduced photosynthetic foliage in a process best defined by vegetation browning (Myers-Smith et al., 2020). Notably, shrub expansion promotes snow accumulation amplifying the impacts of increased precipitation over time (Sturm et al., 2005). Subject to progressive permafrost degradation, the system is likely to undergo shifts towards a wet sedge dominated system following a browning process similar to that observed in our DS site. This may contribute to the slowdown of apparent Arctic greening reported in some regions in recent years (Phoenix and Bjerke, 2016). The strong dependence of plant community structure on snowfall and legacies onto SWC during the snow-free period adds to a building body of knowledge to explain the large spatial heterogeneity observed in these relatively recent phenomena (Berner et al., 2020; Campbell et al., 2021; Heijmans et al., 2022; Phoenix and Treharne, 2022).

Contrary to our initial hypotheses, far from a productivity-driven attenuating effect on climate accompanying shrub expansion, the tight regulation of photosynthetic CO_2 uptake at canopy level limited the response of GPP and the R_{aut}-to-GPP ratio to snow depth. Observed Arctic greening trends over the last decades has been used as an indication of the potential of climate-driven increases in GPP to act as a significant mitigating agent of climate change (Forkel et al., 2016; Myers-Smith et al., 2011; Qian et al., 2010). Our results challenge claims of a large attenuating effect from enhanced GPP and agrees with recent evidence suggesting limited ability of increases in biomass to offset C losses across northern permafrost ecosystems under future climate scenarios (Abbott et al., 2016; Christiansen et al., 2018; McGuire et al., 2018; See et al., 2024; Watts et al., 2021; Zona et al., 2022).

Our results further suggest that the stronger trends in the GPP than in R_{eco} annual amplitudes reported in association with widespread greening across Arctic tundra may be largely explained by constraints on microbial function and activity (Forkel et al., 2016). Seemingly at odds with model predictions of a positive C-climate feedback proportional to warming- and thaw-induced increases in SOC availability and decomposability (Harden et al., 2012; Koven et al., 2015a; Lawrence et al., 2015; Schaefer et al., 2014), concurrent increases in SWC are likely to limit the temperature sensitivity of SOC decomposition rates and reduce seasonal C losses with deeper snow. The dominant role of SWC in driving the C-climate feedback from Arctic tundra is further emphasized by observed exponential increases in CH_4 emissions with deeper snow, which significantly increased the GWP of Arctic tundra despite decreases in C losses.

Recent model ensembles project increases in summer and autumn rainfall accompanying increases in winter snowfall (Bintanja, 2018; McCrystall et al., 2021; Stuefer et al., 2020). Increased rainfall added to snow-and thaw-induced increases in SWC, and latent heat may trigger a hardly reversible positive feedback on permafrost degradation. Severe permafrost degradation under projected changes in precipitation over time spans longer than considered in this study, by promoting soil drainage could suppress CH_4 emissions but accelerate R_{het}, drastically increasing Arctic tundra C losses (Lawrence et al., 2015; Liljedahl et al., 2016; Schädel et al., 2016).

5. Conclusions

We provide empirical evidence of the complex mechanisms governing the response of Arctic tundra to emerging precipitation trends, contributing to closing the gap between model predictions and field observations. Our results reveal key regulatory pathways that, departing from the turnover-driven acceleration vs productivity-driven mitigation framework, may trigger profound alterations of the structure and functioning of Arctic terrestrial ecosystems under future climate scenarios. We further propose a prominent role of the hydrologic system on the fate of permafrost C and suggest that changes in precipitation may be as relevant a climate forcing element as warming in Arctic regions. The direction and magnitude of the derived C-climate feedback, however, will depend on the severity and operating times of the disturbance.

CRediT authorship contribution statement

Elena Blanc-Betes: Writing – review & editing, Writing – original draft, Visualization, Validation, Methodology, Investigation, Formal analysis, Data curation, Conceptualization. **Jeffrey M. Welker:** Writing – review & editing, Funding acquisition, Conceptualization. **Nuria Gomez-Casanovas:** Writing – review & editing, Conceptualization. **Evan H. DeLucia:** Writing – review & editing. **Josep Peñuelas:** Writing – review & editing. **Eduardo Dias de Oliveira:** Writing – review & editing. **Miquel A. Gonzalez-Meler:** Writing – review & editing, Funding acquisition, Conceptualization.

Declaration of competing interest

The authors declare that they have no known competing financial interests or personal relationships that could have appeared to influence the work reported in this paper.

Acknowledgements

This study was made possible by the field assistance of N Van Hoey and B. Thurnhoffer. We are grateful to the Toolik Lake Field Station staff and the CH2MHill Polar Services for their logistical support. This research was funded by the DOE, Terrestrial Ecosystem Science Program (DE-SC 0006607) awarded to MGM and JMW during the sampling period while the experiment was established, maintained initially by NSF Office of Polar Programs Award number 9321730 to JMW, and subsequent NSF Office of Polar Programs awards to JMW 9617643, 0856728, 1504141.

Appendix A. Supplementary data

Supplementary data to this article can be found online at https://doi.org/10.1016/j.scitotenv.2024.178246.

Data availability

Data will be made available on request.

References

Abbott, B.W., Jones, J.B., Schuur, E.A.G., Chapin III, F.S., Bowden, W.B., Bret-Harte, M. S., Epstein, H.E., Flannigan, M.D., Harms, T.K., Hollingsworth, T.N., Mack, M.C., McGuire, A.D., Natali, S.M., Rocha, A.V., Tank, S.E., Turetsky, M.R., Vonk, J.E., Wickland, K.P., Aiken, G.R., Alexander, H.D., Amon, R.M.W., Benscoter, B.W., Bergeron, Yves, Bishop, K., Blarquez, O., Bond-Lamberty, B., Breen, A.L., Buffam, I., Cai, Yihua, Carcaillet, C., Carey, S.K., Chen, J.M., Chen, H.Y.H., Christensen, T.R., Cooper, L.W., Cornelissen, J.H.C., Groot, W.J. de, DeLuca, T.H., Dorrepaal, E., Fetcher, N., Finlay, J.C., Forbes, B.C., French, N.H.F., Gauthier, S., Girardin, M.P., Goetz, S.J., Goldammer, J.G., Gough, L., Grogan, P., Guo, L., Higuera, P.E., Hinzman, L., Hu, F.S., Hugelius, Gustaf, Jafarov, E.E., Jandt, R., Johnstone, J.F., Karlsson, J., Kasischke, E.S., Kattner, Gerhard, Kelly, R., Keuper, F., Kling, G.W., Kortelainen, P., Kouki, J., Kuhry, P., Laudon, Hjalmar, Laurion, I., Macdonald, R.W., Mann, P.J., Martikainen, P.J., McClelland, J.W., Molau, Ulf, Oberbauer, S.F., Olefeldt, D., Paré, D., Parisien, M.-A., Payette, S., Peng, Changhui, Pokrovsky, O.S., Rastetter, E.B., Raymond, P.A., Raynolds, M.K., Rein, G., Reynolds, J.F., Robards, M., Rogers, B.M., Schädel, C., Schaefer, K., Schmidt, I.K., Shvidenko, Anatoly, Sky, J., Spencer, R.G.M., Starr, G., Striegl, R.G., Teisserenc, R., Tranvik, L.J., Virtanen, T., Welker, J.M., Zimov, S., 2016. Biomass offsets little or none of permafrost carbon release from soils, streams, and wildfire: an expert assessment. Environ. Res. Lett. 11, 034014. https://doi.org/10.1088/1748-9326/11/3/034014.

Arens, S.J.T., Sullivan, P.F., Welker, J.M., 2008. Nonlinear responses to nitrogen and strong interactions with nitrogen and phosphorus additions drastically alter the structure and function of a high arctic ecosystem. J. Geophys. Res. Biogeosciences 113, G03S09. https://doi.org/10.1029/2007JG000508.

Bennie, J., Davies, T.W., Cruse, D., Bell, F., Gaston, K.J., 2018. Artificial light at night alters grassland vegetation species composition and phenology. J. Appl. Ecol. 55, 442–450. https://doi.org/10.1111/1365-2664.12927.

Berner, L.T., Massey, R., Jantz, P., Forbes, B.C., Macias-Fauria, M., Myers-Smith, I., Kumpula, T., Gauthier, G., Andreu-Hayles, L., Gaglioti, B.V., Burns, P., Zetterberg, P., D'Arrigo, R., Goetz, S.J., 2020. Summer warming explains widespread but not uniform greening in the Arctic tundra biome. Nat. Commun. 11, 4621. https://doi.org/10.1038/s41467-020-18479-5.

Biasi, C., Rusalimova, O., Meyer, H., Kaiser, C., Wanek, W., Barsukov, P., Junger, H., Richter, A., 2005. Temperature-dependent shift from labile to recalcitrant carbon sources of arctic heterotrophs. Rapid Commun. Mass Spectrom. 19, 1401–1408. https://doi.org/10.1002/rcm.1911.

Biasi, C., Jokinen, S., Marushchak, M.E., Hämäläinen, K., Trubnikova, T., Oinonen, M., Martikainen, P.J., 2014. Microbial respiration in Arctic upland and peat soils as a source of atmospheric carbon dioxide. Ecosystems 17, 112–126. https://doi.org/10.1007/s10021-013-9710-z.

Bintanja, R., 2018. The impact of Arctic warming on increased rainfall. Sci. Rep. 8, 16001. https://doi.org/10.1038/s41598-018-34450-3.

Bintanja, R., Selten, F.M., 2014. Future increases in Arctic precipitation linked to local evaporation and sea-ice retreat. Nature 509, 479–482. https://doi.org/10.1038/nature13259.

Blanc-Betes, E., Welker, J.M., Sturchio, N.C., Chanton, J.P., Gonzalez-Meler, M.A., 2016. Winter precipitation and snow accumulation drive the methane sink or source strength of Arctic tussock tundra. Glob. Change Biol. 22, 2818–2833. https://doi.org/10.1111/gcb.13242.

Bosiö, J., Stiegler, C., Johansson, M., Mbufong, H.N., Christensen, T.R., 2014. Increased photosynthesis compensates for shorter growing season in subarctic tundra—8 years of snow accumulation manipulations. Clim. Change 127, 321–334. https://doi.org/10.1007/s10584-014-1247-4.

Bradford, M.A., Crowther, T.W., 2013. Carbon use efficiency and storage in terrestrial ecosystems. New Phytol. 199, 7–9. https://doi.org/10.1111/nph.12334.

Bret-Harte, M.S., Shaver, G.R., Zoerner, J.P., Johnstone, J.F., Wagner, J.L., Chavez, A.S., Gunkelman, R.F., Lippert, S.C., Laundre, J.A., 2001. Developmental plasticity allows Betula nana to dominate tundra subjected to an altered environment. Ecology 82, 18–32. https://doi.org/10.1890/0012-9658(2001)082[0018:DPABNT]2.0.CO;2.

Bret-Harte, M.S., Shaver, G.R., Chapin, F.S., 2002. Primary and secondary stem growth in arctic shrubs: implications for community response to environmental change. J. Ecol. 90, 251–267. https://doi.org/10.1046/j.1365-2745.2001.00657.x.

Burke, E.J., Hartley, I.P., Jones, C.D., 2012a. Uncertainties in the global temperature change caused by carbon release from permafrost thawing. Cryosphere 6, 1063–1076. https://doi.org/10.5194/tc-6-1063-2012.

Burke, Eleanor J., Jones, C.D., Koven, C.D., 2012b. Estimating the permafrost-carbon climate response in the CMIP5 climate models using a simplified approach. J. Climate 26, 4897–4909. https://doi.org/10.1175/JCLI-D-12-00550.1.

Burke, E.J., Ekici, A., Huang, Y., Chadburn, S.E., Huntingford, C., Ciais, P., Friedlingstein, P., Peng, S., Krinner, G., 2017. Quantifying uncertainties of permafrost carbon–climate feedbacks. Biogeosciences Katlenburg-Lindau 14, 3051–3066. https://doi.org/10.5194/bg-14-3051-2017.

Burke, E.J., Chadburn, S.E., Huntingford, C., Jones, C.D., 2018. CO_2 loss by permafrost thawing implies additional emissions reductions to limit warming to 1.5 or 2 °C. Environ. Res. Lett. 13, 024024. https://doi.org/10.1088/1748-9326/aaa138.

Callaghan, T.V., Johansson, M., Brown, R.D., Groisman, P.Y., Labba, N., Radionov, V., Barry, R.G., Bulygina, O.N., Essery, R.L.H., Frolov, D.M., Golubev, V.N., Grenfell, T. C., Petrushina, M.N., Razuvaev, V.N., Robinson, D.A., Romanov, P., Shindell, D., Shmakin, A.B., Sokratov, S.A., Warren, S., Yang, D., 2011. The changing face of Arctic snow cover: a synthesis of observed and projected changes. AMBIO 40, 17–31. https://doi.org/10.1007/s13280-011-0212-y.

Callaghan, T.V., Cazzolla Gatti, R., Phoenix, G., 2022. The need to understand the stability of arctic vegetation during rapid climate change: an assessment of imbalance in the literature. Ambio 51, 1034–1044. https://doi.org/10.1007/s13280-021-01607-w.

Campbell, T.K.F., Lantz, T.C., Fraser, R.H., Hogan, D., 2021. High Arctic vegetation change mediated by hydrological conditions. Ecosystems 24, 106–121. https://doi.org/10.1007/s10021-020-00506-7.

Carvalhais, N., Forkel, M., Khomik, M., Bellarby, J., Jung, M., Migliavacca, M., Mu, M., Saatchi, S., Santoro, M., Thurner, M., Weber, U., Ahrens, B., Beer, C., Cescatti, A., Randerson, J.T., Reichstein, M., 2014. Global covariation of carbon turnover times with climate in terrestrial ecosystems. Nature 514, 213–217. https://doi.org/10.1038/nature13731.

Chen, G., Yang, Y., Robinson, D., 2013. Allocation of gross primary production in forest ecosystems: allometric constraints and environmental responses. New Phytol. 200, 1176–1186. https://doi.org/10.1111/nph.12426.

Christiansen, Lafreniére Melissa, J., Henry Gregory, H.R., Paul, Grogan, 2018. Long-term deepened snow promotes tundra evergreen shrub growth and summertime ecosystem net CO_2 gain but reduces soil carbon and nutrient pools. Glob. Change Biol. 0. https://doi.org/10.1111/gcb.14084.

Crichton, K.A., Bouttes, N., Roche, D.M., Chappellaz, J., Krinner, G., 2016. Permafrost carbon as a missing link to explain CO_2 changes during the last deglaciation. Nat. Geosci. 9, 683–686. https://doi.org/10.1038/ngeo2793.

Czimczik, C.I., Welker, J.M., 2010. Radiocarbon content of CO_2 respired from high Arctic tundra in Northwest Greenland. Arct. Antarct. Alp. Res. 42, 342–350. https://doi.org/10.1657/1938-4246-42.3.342.

Davidson, E.A., Janssens, I.A., 2006. Temperature sensitivity of soil carbon decomposition and feedbacks to climate change. Nature 440, 165–173. https://doi.org/10.1038/nature04514.

Davidson, E.A., Janssens, I.A., Luo, Y., 2006. On the variability of respiration in terrestrial ecosystems: moving beyond Q10. Glob. Change Biol. 12, 154–164. https://doi.org/10.1111/j.1365-2486.2005.01065.x.

Davidson, E.A., Nepstad, D.C., Ishida, F.Y., Brando, P.M., 2008. Effects of an experimental drought and recovery on soil emissions of carbon dioxide, methane, nitrous oxide, and nitric oxide in a moist tropical forest. Glob. Change Biol. 14, 2582–2590. https://doi.org/10.1111/j.1365-2486.2008.01694.x.

DeLucia, E.H., Drake, J.E., Thomas, R.B., Gonzalez-Meler, M., 2007. Forest carbon use efficiency: is respiration a constant fraction of gross primary production? Glob. Change Biol. 13, 1157–1167. https://doi.org/10.1111/j.1365-2486.2007.01365.x.

DeMarco, J., Mack, M.C., Bret-Harte, M.S., 2014a. Effects of arctic shrub expansion on biophysical vs. biogeochemical drivers of litter decomposition. Ecology 95, 1861–1875. https://doi.org/10.1890/13-2221.1.

DeMarco, J., Mack, M.C., Bret-Harte, M.S., Burton, M., Shaver, G.R., 2014b. Long-term experimental warming and nutrient additions increase productivity in tall deciduous shrub tundra. Ecosphere 5, 1–22. https://doi.org/10.1890/ES13-00281.1.

Deslippe, J.R., Simard, S.W., 2011. Below-ground carbon transfer among Betula nana may increase with warming in Arctic tundra. New Phytol. 192, 689–698. https://doi.org/10.1111/j.1469-8137.2011.03835.x.

Elmendorf, S.C., Henry, G.H.R., Hollister, R.D., Björk, R.G., Bjorkman, A.D., Callaghan, T.V., Collier, L.S., Cooper, E.J., Cornelissen, J.H.C., Day, T.A., Fosaa, A. M., Gould, W.A., Grétarsdóttir, J., Harte, J., Hermanutz, L., Hik, D.S., Hofgaard, A., Jarrad, F., Jónsdóttir, I.S., Keuper, F., Klanderud, K., Klein, J.A., Koh, S., Kudo, G., Lang, S.I., Loewen, V., May, J.L., Mercado, J., Michelsen, A., Molau, U., Myers-Smith, I.H., Oberbauer, S.F., Pieper, S., Post, E., Rixen, C., Robinson, C.H., Schmidt, N.M., Shaver, G.R., Stenström, A., Tolvanen, A., Totland, Ø., Troxler, T., Wahren, C.-H., Webber, P.J., Welker, J.M., Wookey, P.A., 2012a. Global assessment of experimental climate warming on tundra vegetation: heterogeneity over space and time. Ecol. Lett. 15, 164–175. https://doi.org/10.1111/j.1461-0248.2011.01716.x.

Elmendorf, S.C., Henry, G.H.R., Hollister, R.D., Björk, R.G., Boulanger-Lapointe, N., Cooper, E.J., Cornelissen, J.H.C., Day, T.A., Dorrepaal, E., Elumeeva, T.G., Gill, M., Gould, W.A., Harte, J., Hik, D.S., Hofgaard, A., Johnson, D.R., Johnstone, J.F., Jónsdóttir, I.S., Jorgenson, J.C., Klanderud, K., Klein, J.A., Koh, S., Kudo, G., Lara, M., Lévesque, E., Magnússon, B., May, J.L., Mercado-Diaz, J.A., Michelsen, A., Molau, U., Myers-Smith, I.H., Oberbauer, S.F., Onipchenko, V.G., Rixen, C., Martin Schmidt, N., Shaver, G.R., Spasojevic, M.J., Þórhallsdóttir, Þ.E., Tolvanen, A., Troxler, T., Tweedie, C.E., Villareal, S., Wahren, C.-H., Walker, X., Webber, P.J., Welker, J.M., Wipf, S., 2012b. Plot-scale evidence of tundra vegetation change and links to recent summer warming. Nat. Clim. Change 2, 453–457. https://doi.org/10.1038/nclimate1465.

Environ. Data Center, TFS, 2023. Environmental Data Center [WWW Document]. Meteorol. Monit. Program Toolik Alsk. Toolik Field Stn. Inst. Arct. Biol. Univ. Alsk. Fairbanks Fairbanks AK 99775. URL https://www.uaf.edu/toolik/edc/monitoring/abiotic/met-data-query.php.

Feng, J., Wang, C., Lei, J., Yang, Y., Yan, Q., Zhou, X., Tao, X., Ning, D., Yuan, M.M., Qin, Y., Shi, Z.J., Guo, X., He, Z., Van Nostrand, J.D., Wu, L., Bracho-Garillo, R.G., Penton, C.R., Cole, J.R., Konstantinidis, K.T., Luo, Y., Schuur, E.A.G., Tiedje, J.M., Zhou, J., 2020. Warming-induced permafrost thaw exacerbates tundra soil carbon decomposition mediated by microbial community. Microbiome 8, 3. https://doi.org/10.1186/s40168-019-0778-3.

Forbes, B.C., 2015. Arctic vegetation cover: patterns, processes and expected change. In: Evengård, B., Larsen, J.N., Paasche, Ø. (Eds.), The New Arctic. Springer International Publishing, pp. 117–132. https://doi.org/10.1007/978-3-319-17602-4_9.

Forkel, M., Carvalhais, N., Rödenbeck, C., Keeling, R., Heimann, M., Thonicke, K., Zaehle, S., Reichstein, M., 2016. Enhanced seasonal CO_2 exchange caused by amplified plant productivity in northern ecosystems. Science 351, 696–699. https://doi.org/10.1126/science.aac4971.

Gentsch, N., Wild, B., Mikutta, R., Čapek, P., Diáková, K., Schrumpf, M., Turner, S., Minnich, C., Schaarschmidt, F., Shibistova, O., Schnecker, J., Urich, T., Gittel, A., Šantrůčková, H., Bárta, J., Lashchinskiy, N., Fuß, R., Richter, A., Guggenberger, G., 2018. Temperature response of permafrost soil carbon is attenuated by mineral protection. Glob. Change Biol. 24, 3401–3415. https://doi.org/10.1111/gcb.14316.

Gisnås, K., Westermann, S., Schuler, T.V., Litherland, T., Isaksen, K., Boike, J., Etzelmüller, B., 2014. A statistical approach to represent small-scale variability of permafrost temperatures due to snow cover. The Cryosphere 8, 2063–2074. https://doi.org/10.5194/tc-8-2063-2014.

Gomez-Casanovas, N., Matamala, R., Cook, D.R., Gonzalez-Meler, M.A., 2012. Net ecosystem exchange modifies the relationship between the autotrophic and heterotrophic components of soil respiration with abiotic factors in prairie grasslands. Glob. Change Biol. 18, 2532–2545.

Gomez-Casanovas, N., Anderson-Teixeira, K., Zeri, M., Bernacchi, C.J., DeLucia, E.H., 2013. Gap filling strategies and error in estimating annual soil respiration. Glob. Change Biol. 19, 1941–1952. https://doi.org/10.1111/gcb.12127.

Grant, R.F., 2015. Ecosystem CO_2 and CH_4 exchange in a mixed tundra and a fen within a hydrologically diverse Arctic landscape: 2. Modeled impacts of climate change. J. Geophys. Res. Biogeosciences 120, 2014JG002889. https://doi.org/10.1002/2014JG002889.

Groendahl, L., Friborg, T., Soegaard, H., 2007. Temperature and snow-melt controls on interannual variability in carbon exchange in the high Arctic. Theor. Appl. Climatol. 88, 111–125. https://doi.org/10.1007/s00704-005-0228-y.

Grogan, P., Chapin III, F.S., 1999. Arctic soil respiration: effects of climate and vegetation depend on season. Ecosystems 2, 451–459. https://doi.org/10.1007/s100219900093.

Grogan, P., Chapin III, F.S., 2000. Initial effects of experimental warming on above- and belowground components of net ecosystem CO_2 exchange in arctic tundra. Oecologia 125, 512–520. https://doi.org/10.1007/s004420000490.

Harden, J.W., Koven, C.D., Ping, C.-L., Hugelius, G., David McGuire, A., Camill, P., Jorgenson, T., Kuhry, P., Michaelson, G.J., O'Donnell, J.A., Schuur, E.A.G., Tarnocai, C., Johnson, K., Grosse, G., 2012. Field information links permafrost carbon to physical vulnerabilities of thawing. Geophys. Res. Lett. 39, L15704. https://doi.org/10.1029/2012GL051958.

Heijmans, M.M.P.D., Magnússon, R.Í., Lara, M.J., Frost, G.V., Myers-Smith, I.H., van Huissteden, J., Jorgenson, M.T., Fedorov, A.N., Epstein, H.E., Lawrence, D.M., Limpens, J., 2022. Tundra vegetation change and impacts on permafrost. Nat. Rev. Earth Environ. 3, 68–84. https://doi.org/10.1038/s43017-021-00233-0.

Hicks Pries, C.E., Schuur, E.A.G., Natali, S.M., Crummer, K.G., 2016. Old soil carbon losses increase with ecosystem respiration in experimentally thawed tundra. Nat. Clim. Change 6, 214–218. https://doi.org/10.1038/nclimate2830.

Hobbie, S.E., 1996. Temperature and plant species control over litter decomposition in Alaskan tundra. Ecological monographs 66, 503–522. https://doi.org/10.2307/2963492.

Hopkins, F., Gonzalez-Meler, M.A., Flower, C.E., Lynch, D.J., Czimczik, C., Tang, J., Subke, J.-A., 2013. Ecosystem-level controls on root-rhizosphere respiration. New Phytol. 199, 339–351. https://doi.org/10.1111/nph.12271.

Huemmrich, K.F., Kinoshita, G., Gamon, J.A., Houston, S., Kwon, H., Oechel, W.C., 2010. Tundra carbon balance under varying temperature and moisture regimes. J. Geophys. Res. Biogeosciences 115, G00I02. https://doi.org/10.1029/2009JG001237.

Hugelius, G., Strauss, J., Zubrzycki, S., Harden, J.W., Schuur, E., Ping, C.-L., Schirrmeister, L., Grosse, G., Michaelson, G.J., Koven, C.D., et al., 2014. Improved estimates show large circumpolar stocks of permafrost carbon while quantifying substantial uncertainty ranges and identifying remaining data gaps. Biogeosci. Discuss. 11, 4771–4822.

Hursh, A., Ballantyne, A., Cooper, L., Maneta, M., Kimball, J., Watts, J., 2017. The sensitivity of soil respiration to soil temperature, moisture, and carbon supply at the global scale. Glob. Change Biol. 23, 2090–2103. https://doi.org/10.1111/gcb.13489.

Ives, S.L., Sullivan, P.F., Dial, R., Berg, E.E., Welker, J.M., 2013. CO_2 exchange along a hydrologic gradient in the Kenai Lowlands, AK: feedback implications of wetland drying and vegetation succession. Ecohydrology 6, 38–50. https://doi.org/10.1002/eco.274.

Jespersen, R.G., Anderson-Smith, M., Sullivan, P.F., Dial, R.J., Welker, J.M., 2023. NDVI changes in the Arctic: functional significance in the moist acidic tundra of Northern Alaska. PloS One 18, e0285030. https://doi.org/10.1371/journal.pone.0285030.

Johansson, M., Callaghan, T.V., Bosiö, J., Åkerman, H.J., Jackowicz-Korczynski, M., Christensen, T.R., 2013. Rapid responses of permafrost and vegetation to experimentally increased snow cover in sub-arctic Sweden. Environ. Res. Lett. 8, 035025. https://doi.org/10.1088/1748-9326/8/3/035025.

Jones, M.H., Fahnestock, J.T., Walker, D.A., Walker, M.D., Welker, J.M., 1998. Carbon dioxide fluxes in moist and dry Arctic tundra during the snow-free season: responses to increases in summer temperature and winter snow accumulation. Arct. Alp. Res. 30, 373–380. https://doi.org/10.2307/1552009.

Kelsey, K.C., Pedersen, S.H., Leffler, A.J., Sexton, J.O., Feng, M., Welker, J.M., 2021. Winter snow and spring temperature have differential effects on vegetation phenology and productivity across Arctic plant communities. Glob. Change Biol. 27, 1572–1586. https://doi.org/10.1111/gcb.15505.

Khani, H.M., Kinnard, C., Lévesque, E., 2022. Historical trends and projections of snow cover over the high Arctic: a review. Water 14, 587. https://doi.org/10.3390/w14040587.

Knoblauch, C., Beer, C., Liebner, S., Grigoriev, M.N., Pfeiffer, E.-M., 2018. Methane production as key to the greenhouse gas budget of thawing permafrost. Nat. Clim. Change 8, 309–312. https://doi.org/10.1038/s41558-018-0095-z.

Kohler, J., Brandt, O., Johansson, M., Callaghan, T., 2006. A long-term Arctic snow depth record from Abisko, northern Sweden, 1913–2004. Polar Res. 25, 91–113. https://doi.org/10.3402/polar.v25i2.6240.

Koven, C.D., Riley, W.J., Stern, A., 2013. Analysis of permafrost thermal dynamics and response to climate change in the CMIP5 earth system models. J. Climate 26, 1877–1900. https://doi.org/10.1175/JCLI-D-12-00228.1.

Koven, C.D., Chambers, J.Q., Georgiou, K., Knox, R., Negron-Juarez, R., Riley, W.J., Arora, V.K., Brovkin, V., Friedlingstein, P., Jones, C.D., 2015a. Controls on Terrestrial Carbon Feedbacks by Productivity Versus Turnover in the CMIP5 Earth System Models. https://doi.org/10.5194/bg-12-5211-2015.

Koven, C.D., Schuur, E.a.G., Schädel, C., Bohn, T.J., Burke, E.J., Chen, G., Chen, X., Ciais, P., Grosse, G., Harden, J.W., Hayes, D.J., Hugelius, G., Jafarov, E.E., Krinner, G., Kuhry, P., Lawrence, D.M., MacDougall, A.H., Marchenko, S.S., McGuire, A.D., Natali, S.M., Nicolsky, D.J., Olefeldt, D., Peng, S., Romanovsky, V.E., Schaefer, K.M., Strauss, J., Treat, C.C., Turetsky, M., 2015b. A simplified, data-constrained approach to estimate the permafrost carbon–climate feedback. Phil. Trans. R. Soc. A 373, 20140423. https://doi.org/10.1098/rsta.2014.0423.

Kuzyakov, Y., 2006. Sources of CO_2 efflux from soil and review of partitioning methods. Soil Biol. Biochem. 38, 425–448. https://doi.org/10.1016/j.soilbio.2005.08.020.

Kwon, H.-J., Oechel, W.C., Zulueta, R.C., Hastings, S.J., 2006. Effects of climate variability on carbon sequestration among adjacent wet sedge tundra and moist tussock tundra ecosystems. J. Geophys. Res. Biogeo. 111. https://doi.org/10.1029/2005JG000036.

La Puma, I.P., Philippi, T.E., Oberbauer, S.F., 2007. Relating NDVI to ecosystem CO_2 exchange patterns in response to season length and soil warming manipulations in arctic Alaska. Remote Sens. Environ. 109, 225–236. https://doi.org/10.1016/j.rse.2007.01.001.

Lasslop, G., Reichstein, M., Detto, M., Richardson, A.D., Baldocchi, D.D., 2010. Comment on Vickers et al.: self-correlation between assimilation and respiration resulting from flux partitioning of eddy-covariance CO_2 fluxes. Agric. For. Meteorol. 150, 312–314. https://doi.org/10.1016/j.agrformet.2009.11.003.

Lawrence, D.M., Slater, A.G., 2010. The contribution of snow condition trends to future ground climate. Climate Dynam. 34, 969–981. https://doi.org/10.1007/s00382-009-0537-4.

Lawrence, D.M., Koven, C.D., Swenson, S.C., Riley, W.J., Slater, A.G., 2015. Permafrost thaw and resulting soil moisture changes regulate projected high-latitude CO_2 and CH_4 emissions. Environ. Res. Lett. 10, 094011. https://doi.org/10.1088/1748-9326/10/9/094011.

Leffler, A.J., Klein, E.S., Oberbauer, S.F., Welker, J.M., 2016. Coupled long-term summer warming and deeper snow alters species composition and stimulates gross primary productivity in tussock tundra. Oecologia 181, 287–297. https://doi.org/10.1007/s00442-015-3543-8.

Liljedahl, A.K., Boike, J., Daanen, R.P., Fedorov, A.N., Frost, G.V., Grosse, G., Hinzman, L.D., Iijma, Y., Jorgenson, J.C., Matveyeva, N., Necsoiu, M., Raynolds, M. K., Romanovsky, V.E., Schulla, J., Tape, K.D., Walker, D.A., Wilson, C.J., Yabuki, H., Zona, D., 2016. Pan-Arctic ice-wedge degradation in warming permafrost and its influence on tundra hydrology. Nat. Geosci. 9, 312–318. https://doi.org/10.1038/ngeo2674.

Liu, Y., Hansen, B.U., Elberling, B., Westergaard-Nielsen, A., 2023. Snow depth and the associated offset in ground temperatures in a landscape manipulated with snow-fences. Geoderma 438, 116632. https://doi.org/10.1016/j.geoderma.2023.116632.

Lloyd, J., Taylor, J.A., 1994. On the temperature dependence of soil respiration. Funct. Ecol. 8, 315–323. https://doi.org/10.2307/2389824.

Lund, M., Lafleur, P.M., Roulet, N.T., Lindroth, A., Christensen, T.R., Aurela, M., Chojnicki, B.H., Flanagan, L.B., Humphreys, E.R., Laurila, T., Oechel, W.C., Olejnik, J., Rinne, J., Schubert, P., Nilsson, M.B., 2010. Variability in exchange of CO_2 across 12 northern peatland and tundra sites. Glob. Change Biol. 16, 2436–2448. https://doi.org/10.1111/j.1365-2486.2009.02104.x.

Luo, Y., Melillo, J., Niu, S., Beier, C., Clark, J.S., Classen, A.T., Davidson, E., Dukes, J.S., Evans, R.D., Field, C.B., Czimczik, C.I., Keller, M., Kimball, B.A., Kueppers, L.M., Norby, R.J., Pelini, S.L., Pendall, E., Rastetter, E., Six, J., Smith, M., Tjoelker, M.G., Torn, M.S., 2011. Coordinated approaches to quantify long-term ecosystem dynamics in response to global change. Glob. Change Biol. 17, 843–854. https://doi.org/10.1111/j.1365-2486.2010.02265.x.

Lupascu, M., Welker, J.M., Xu, X., Czimczik, C.I., 2014. Rates and radiocarbon content of summer ecosystem respiration in response to long-term deeper snow in the High Arctic of NW Greenland. J. Geophys. Res. Biogeosciences 119, 2013JG002494. https://doi.org/10.1002/2013JG002494.

Mack, M.C., Schuur, E.A.G., Bret-Harte, M.S., Shaver, G.R., Chapin, F.S., 2004. Ecosystem carbon storage in arctic tundra reduced by long-term nutrient fertilization. Nature 431, 440–443. https://doi.org/10.1038/nature02887.

Mauritz, M., Bracho, R., Celis, G., Hutchings, J., Natali, S.M., Pegoraro, E., Salmon, V.G., Schädel, C., Webb, E.E., Schuur, E.A.G., 2017. Non-linear CO_2 flux response to seven years of experimentally induced permafrost thaw. Glob. Change Biol. https://doi.org/10.1111/gcb.13661 n/a-n/a.

McConnell, N.A., Turetsky, M.R., McGuire, A.D., Kane, E.S., Waldrop, M.P., Harden, J. W., 2013. Controls on ecosystem and root respiration across a permafrost and wetland gradient in interior Alaska. Environ. Res. Lett. 8, 045029. https://doi.org/10.1088/1748-9326/8/4/045029.

McCrystall, M.R., Stroeve, J., Serreze, M., Forbes, B.C., Screen, J.A., 2021. New climate models reveal faster and larger increases in Arctic precipitation than previously projected. Nat. Commun. 12, 6765. https://doi.org/10.1038/s41467-021-27031-y.

McGuire, A.D., Christensen, T.R., Hayes, D., Heroult, A., Euskirchen, E., Yi, Y., Kimball, J.S., Koven, C., Lafleur, P., Miller, P.A., Oechel, W., Peylin, P., Williams, M., 2012. An assessment of the carbon balance of arctic tundra: comparisons among observations, process models, and atmospheric inversions. Biogeosci. Discuss. 9, 4543–4594. https://doi.org/10.5194/bgd-9-4543-2012.

McGuire, A.D., Koven, C., Lawrence, D.M., Clein, J.S., Xia, J., Beer, C., Burke, E., Chen, G., Chen, X., Delire, C., Jafarov, E., MacDougall, A.H., Marchenko, S., Nicolsky, D., Peng, S., Rinke, A., Saito, K., Zhang, W., Alkama, R., Bohn, T.J., Ciais, P., Decharme, B., Ekici, A., Gouttevin, I., Hajima, T., Hayes, D.J., Ji, D., Krinner, G., Lettenmaier, D.P., Luo, Y., Miller, P.A., Moore, J.C., Romanovsky, V., Schädel, C., Schaefer, K., Schuur, E.A.G., Smith, B., Sueyoshi, T., Zhuang, Q., 2016. Variability in the sensitivity among model simulations of permafrost and carbon dynamics in the permafrost region between 1960 and 2009. Global Biogeochem. Cycles, 2016GB005405. https://doi.org/10.1002/2016GB005405.

McGuire, A.D., Lawrence, D.M., Koven, C., Clein, J.S., Burke, E., Chen, G., Jafarov, E., MacDougall, A.H., Marchenko, S., Nicolsky, D., Peng, S., Rinke, A., Ciais, P., Gouttevin, I., Hayes, D.J., Ji, D., Krinner, G., Moore, J.C., Romanovsky, V., Schädel, C., Schaefer, K., Schuur, E.A.G., Zhuang, Q., 2018. Dependence of the evolution of carbon dynamics in the northern permafrost region on the trajectory of climate change. Proc. Natl. Acad. Sci., 201719903 https://doi.org/10.1073/pnas.1719903115.

Mekonnen, Z.A., Riley, W.J., Grant, R.F., 2018. 21st century tundra shrubification could enhance net carbon uptake of North America Arctic tundra under an RCP8.5 climate trajectory. Environ. Res. Lett. 13, 054029. https://doi.org/10.1088/1748-9326/aabf28.

Mekonnen, Z.A., Riley, W.J., Berner, L.T., Bouskill, N.J., Torn, M.S., Iwahana, G., Breen, A.L., Myers-Smith, I.H., Criado, M.G., Liu, Y., Euskirchen, E.S., Goetz, S.J., Mack, M.C., Grant, R.F., 2021. Arctic tundra shrubification: a review of mechanisms and impacts on ecosystem carbon balance. Environ. Res. Lett. 16, 053001. https://doi.org/10.1088/1748-9326/abf28b.

Mikan, C.J., Schimel, J.P., Doyle, A.P., 2002. Temperature controls of microbial respiration in arctic tundra soils above and below freezing. Soil Biol. Biochem. 34, 1785–1795. https://doi.org/10.1016/S0038-0717(02)00168-2.

Miller, P.A., Smith, B., 2012. Modelling tundra vegetation response to recent Arctic warming. AMBIO 41, 281–291. https://doi.org/10.1007/s13280-012-0306-1.

Mishra, U., Hugelius, G., Shelef, E., Yang, Y., Strauss, J., Lupachev, A., Harden, J.W., Jastrow, J.D., Ping, C.-L., Riley, W.J., Schuur, E.A.G., Matamala, R., Siewert, M., Nave, L.E., Koven, C.D., Fuchs, M., Palmtag, J., Kuhry, P., Treat, C.C., Zubrzycki, S., Hoffman, F.M., Elberling, B., Camill, P., Veremeeva, A., Orr, A., 2021. Spatial heterogeneity and environmental predictors of permafrost region soil organic carbon stocks. Sci. Adv. 7, eaaz5236. https://doi.org/10.1126/sciadv.aaz5236.

Morgner, E., Elberling, B., Strebel, D., Cooper, E.J., 2010. The importance of winter in annual ecosystem respiration in the high Arctic: effects of snow depth in two vegetation types. Polar Res. 29, 58–74. https://doi.org/10.1111/j.1751-8369.2010.00151.x.

Mudryk, L., Elias Chereque, A., Derksen, C., Luojus, K., Decharme, B., 2022. Arctic Report Card 2022: Terrestrial Snow Cover. NOAA technical report OAR ARC. https://doi.org/10.25923/YXS5-6C72.

Myers-Smith, I.H., Hik, D.S., 2013. Shrub canopies influence soil temperatures but not nutrient dynamics: an experimental test of tundra snow–shrub interactions. Ecol. Evol. 3, 3683–3700. https://doi.org/10.1002/ece3.710.

Myers-Smith, I.H., Forbes, B.C., Wilmking, M., Hallinger, M., Lantz, T., Blok, D., Tape, K. D., Macias-Fauria, M., Sass-Klaassen, U., Lévesque, E., Boudreau, S., Ropars, P., Hermanutz, Luise, Trant, A., Collier, L.S., Weijers, S., Rozema, J., Rayback, S.A., Schmidt, N.M., Schaepman-Strub, G., Wipf, S., Rixen, C., Ménard, C.B., Venn, Susanna, Goetz, S., Andreu-Hayles, L., Elmendorf, S., Ravolainen, V., Welker, J., Grogan, Paul, Epstein, H.E., Hik, D.S., 2011. Shrub expansion in tundra ecosystems: dynamics, impacts and research priorities. Environ. Res. Lett. 6, 045509. https://doi.org/10.1088/1748-9326/6/4/045509.

Myers-Smith, I.H., Kerby, J.T., Phoenix, G.K., Bjerke, J.W., Epstein, H.E., Assmann, J.J., John, C., Andreu-Hayles, L., Angers-Blondin, S., Beck, P.S.A., Berner, L.T., Bhatt, U. S., Bjorkman, A.D., Blok, D., Bryn, A., Christiansen, C.T., Cornelissen, J.H.C., Cunliffe, A.M., Elmendorf, S.C., Forbes, B.C., Goetz, S.J., Hollister, R.D., de Jong, R., Loranty, M.M., Macias-Fauria, M., Maseyk, K., Normand, S., Olofsson, J., Parker, T. C., Parmentier, F.-J.W., Post, E., Schaepman-Strub, G., Stordal, F., Sullivan, P.F., Thomas, H.J.D., Tømmervik, H., Treharne, R., Tweedie, C.E., Walker, D.A., Wilmking, M., Wipf, S., 2020. Complexity revealed in the greening of the Arctic. Nat. Clim. Change 10, 106–117. https://doi.org/10.1038/s41558-019-0688-1.

Myhre, G., Shindell, D., Bréon, F.M., Collins, W., Fuglestvedt, J., Huang, J., Koch, D., Lamarque, J.F., Lee, D., Mendoza, B., et al., 2013. Anthropogenic and natural radiative forcing. Clim. Change 658–740.

Osterkamp, T.E., 2007. Causes of warming and thawing permafrost in Alaska. EOS Trans. Am. Geophys. Union 88, 522–523. https://doi.org/10.1029/2007EO480002.

Pattison, R.R., Welker, J.M., 2014. Differential ecophysiological response of deciduous shrubs and a graminoid to long-term experimental snow reductions and additions in moist acidic tundra, Northern Alaska. Oecologia 174, 339–350. https://doi.org/10.1007/s00442-013-2777-6.

Pedersen, S.H., Bentzen, T.W., Reinking, A.K., Liston, G.E., Elder, K., Lenart, E.A., Prichard, A.K., Welker, J.M., 2021. Quantifying effects of snow depth on caribou winter range selection and movement in Arctic Alaska. Mov. Ecol. 9, 48. https://doi.org/10.1186/s40462-021-00276-4.

Pedron, S.A., Jespersen, R.G., Xu, X., Khazindar, Y., Welker, J.M., Czimczik, C.I., 2023. More snow accelerates legacy carbon emissions from Arctic permafrost. AGU Adv. 4, e2023AV000942. https://doi.org/10.1029/2023AV000942.

Phoenix, G.K., Bjerke, J.W., 2016. Arctic browning: extreme events and trends reversing arctic greening. Glob. Change Biol. 22, 2960–2962. https://doi.org/10.1111/gcb.13261.

Phoenix, G.K., Treharne, R., 2022. Arctic greening and browning: challenges and a cascade of complexities. Glob. Change Biol. 28, 3481–3483. https://doi.org/10.1111/gcb.16118.

Qian, H., Joseph, R., Zeng, N., 2010. Enhanced terrestrial carbon uptake in the northern high latitudes in the 21st century from the coupled carbon cycle climate model intercomparison project model projections. Glob. Change Biol. 16, 641–656. https://doi.org/10.1111/j.1365-2486.2009.01989.x.

Ren, S., Ding, J., Yan, Z., Cao, Y., Li, J., Wang, Y., Liu, D., Zeng, H., Wang, T., 2020. Higher temperature sensitivity of soil C release to atmosphere from northern permafrost soils as indicated by a meta-analysis. Global Biogeochem. Cycles 34, e2020GB006688. https://doi.org/10.1029/2020GB006688.

Rixen, C., Freppaz, M., Stoeckli, V., Huovinen, C., Huovinen, K., Wipf, S., 2008. Altered snow density and chemistry change soil nitrogen mineralization and plant growth. Arct. Antarct. Alp. Res. 40, 568–575. https://doi.org/10.1657/1523-0430(07-044)[RIXEN]2.0.CO;2.

Rixen, C., Høye, T.T., Macek, P., Aerts, R., Alatalo, J.M., Anderson, J.T., Arnold, P.A., Barrio, I.C., Bjerke, J.W., Björkman, M.P., Blok, D., Blume-Werry, G., Boike, J., Bokhorst, S., Carbognani, M., Christiansen, C.T., Convey, P., Cooper, E.J., Cornelissen, J.H.C., Coulson, S.J., Dorrepaal, E., Elberling, B., Elmendorf, S.C., Elphinstone, C., Forte, T.G.W., Frei, E.R., Geange, S.R., Gehrmann, F., Gibson, C., Grogan, P., Halbritter, A.H., Harte, J., Henry, G.H.R., Inouye, D.W., Irwin, R.E., Jespersen, G., Jónsdóttir, I.S., Jung, J.Y., Klinges, D.H., Kudo, G., Lämsä, J., Lee, H., Lembrechts, J.J., Lett, S., Lynn, J.S., Mann, H.M.R., Mastepanov, M., Morse, J., Myers-Smith, I.H., Olofsson, J., Paavola, R., Petraglia, A., Phoenix, G.K., Semenchuk, P., Siewert, M.B., Slatyer, R., Spasojevic, M.J., Suding, K., Sullivan, P., Thompson, K.L., Väisänen, M., Vandvik, V., Venn, S., Walz, J., Way, R., Welker, J.M., Wipf, S., Zong, S., 2022. Winters are changing: snow effects on Arctic and alpine tundra ecosystems. Arct. Sci. 8, 572–608. https://doi.org/10.1139/as-2020-0058.

Romanovsky, V.E., Smith, S.L., Christiansen, H.H., 2010. Permafrost thermal state in the polar Northern Hemisphere during the international polar year 2007–2009: a synthesis. Permafr. Periglac. Process. 21, 106–116. https://doi.org/10.1002/ppp.689.

Salmon, V.G., Soucy, P., Mauritz, M., Celis, G., Natali, S.M., Mack, M.C., Schuur, E.A.G., 2016. Nitrogen availability increases in a tundra ecosystem during five years of experimental permafrost thaw. Glob. Change Biol. 22, 1927–1941. https://doi.org/10.1111/gcb.13204.

Schädel, C., Bader, M.K.-F., Schuur, E.A.G., Biasi, C., Bracho, R., Čapek, P., De Baets, S., Diáková, K., Ernakovich, J., Estop-Aragones, C., Graham, D.E., Hartley, I.P., Iversen, C.M., Kane, E., Knoblauch, C., Lupascu, M., Martikainen, P.J., Natali, S.M., Norby, R.J., O'Donnell, J.A., Chowdhury, T.R., Šantrůčková, H., Shaver, G., Sloan, V. L., Treat, C.C., Turetsky, M.R., Waldrop, M.P., Wickland, K.P., 2016. Potential carbon emissions dominated by carbon dioxide from thawed permafrost soils. Nat. Clim. Change 6, 950–953. https://doi.org/10.1038/nclimate3054.

Schädel, C., Koven, C.D., Lawrence, D.M., Celis, G., Garnello, A.J., Hutchings, Jack, Mauritz, M., Natali, S.M., Pegoraro, E., Rodenhizer, H., Salmon, V.G., Taylor, M.A., Webb, E.E., Wieder, W.R., Schuur, E.A., 2018. Divergent patterns of experimental and model-derived permafrost ecosystem carbon dynamics in response to Arctic warming. Environ. Res. Lett. 13, 105002. https://doi.org/10.1088/1748-9326/aae0ff.

Schädel, C., Rogers, B.M., Lawrence, D.M., Koven, C.D., Brovkin, V., Burke, E.J., Genet, H., Huntzinger, D.N., Jafarov, E., McGuire, A.D., Riley, W.J., Natali, S.M., 2024. Earth system models must include permafrost carbon processes. Nat. Clim. Change 14, 114–116. https://doi.org/10.1038/s41558-023-01909-9.

Schaefer, K., Zhang, T., Bruhwiler, L., Barrett, A.P., 2011. Amount and timing of permafrost carbon release in response to climate warming. Tellus B 63, 165–180. https://doi.org/10.1111/j.1600-0889.2011.00527.x.

Schaefer, K., Lantuit, H., Romanovsky, V.E., Schuur, E.A.G., Witt, R., 2014. The impact of the permafrost carbon feedback on global climate. Environ. Res. Lett. 9, 085003. https://doi.org/10.1088/1748-9326/9/8/085003.

Schimel, J.P., Bilbrough, C., Welker, J.M., 2004. Increased snow depth affects microbial activity and nitrogen mineralization in two Arctic tundra communities. Soil Biol. Biochem. 36, 217–227. https://doi.org/10.1016/j.soilbio.2003.09.008.

Schuur, E.a.G., McGuire, A.D., Schädel, C., Grosse, G., Harden, J.W., Hayes, D.J., Hugelius, G., Koven, C.D., Kuhry, P., Lawrence, D.M., Natali, S.M., Olefeldt, D., Romanovsky, V.E., Schaefer, K., Turetsky, M.R., Treat, C.C., Vonk, J.E., 2015. Climate change and the permafrost carbon feedback. Nature 520, 171–179. https://doi.org/10.1038/nature14338.

Schuur, E.A.G., Abbott, B.W., Commane, R., Ernakovich, J., Euskirchen, E., Hugelius, G., Grosse, G., Jones, M., Koven, C., Leshyk, V., Lawrence, D., Loranty, M.M., Mauritz, M., Olefeldt, D., Natali, S., Rodenhizer, H., Salmon, V., Schädel, C., Strauss, J., Treat, C., Turetsky, M., 2022. Permafrost and climate change: carbon cycle feedbacks from the warming Arctic. Annu. Rev. Env. Resour. 47, 343–371. https://doi.org/10.1146/annurev-environ-012220-011847.

See, C.R., Virkkala, A.-M., Natali, S.M., Rogers, B.M., Mauritz, M., Biasi, C., Bokhorst, S., Boike, J., Bret-Harte, M.S., Celis, G., Chae, N., Christensen, T.R., Murner (Connon), S.J., Dengel, S., Dolman, H., Edgar, C.W., Elberling, B., Emmerton, C.A., Euskirchen, E.S., Göckede, M., Grelle, A., Heffernan, L., Helbig, M., Holl, D., Humphreys, E., Iwata, H., Järveoja, J., Kobayashi, H., Kochendorfer, J., Kolari, P., Kotani, A., Kutzbach, L., Kwon, M.J., Lathrop, E.R., López-Blanco, E., Mammarella, I., Marushchak, M.E., Mastepanov, M., Matsuura, Y., Merbold, L., Meyer, G., Minions, C., Nilsson, M.B., Nojeim, J., Oberbauer, S.F., Olefeldt, D., Park, S.-J., Parmentier, F.-J.W., Peichl, M., Peter, D., Petrov, R., Poyatos, R., Prokushkin, A.S., Quinton, W., Rodenhizer, H., Sachs, T., Savage, K., Schulze, C., Sjögersten, S., Sonnentag, O., St. Louis, V.L., Torn, M.S., Tuittila, E.-S., Ueyama, M., Varlagin, A., Voigt, C., Watts, J.D., Zona, D., Zyryanov, V.I., Schuur, E.A.G., 2024. Decadal increases in carbon uptake offset by respiratory losses across northern permafrost ecosystems. Nat. Clim. Change 1–10. https://doi.org/10.1038/s41558-024-02057-4.

Semenchuk, P.R., Elberling, B., Amtorp, C., Winkler, J., Rumpf, S., Michelsen, A., Cooper, E.J., 2015. Deeper snow alters soil nutrient availability and leaf nutrient status in high Arctic tundra. Biogeochemistry 124, 81–94. https://doi.org/10.1007/s10533-015-0082-7.

Sharp, E.D., Sullivan, P.F., Steltzer, H., Csank, A.Z., Welker, J.M., 2013. Complex carbon cycle responses to multi-level warming and supplemental summer rain in the high Arctic. Glob. Change Biol. 19, 1780–1792. https://doi.org/10.1111/gcb.12149.

Shaver, G.R., Bret-Harte, M.S., Jones, M.H., Johnstone, J., Gough, L., Laundre, J., Chapin, F.S., 2001. Species composition interacts with fertilizer to control long-term change in tundra productivity. Ecology 82, 3163–3181. https://doi.org/10.1890/0012-9658(2001)082[3163:SCIWFT]2.0.CO;2.

Shaver, G.R., Street, L.E., Rastetter, E.B., Van Wijk, M.T., Williams, M., 2007. Functional convergence in regulation of net CO_2 flux in heterogeneous tundra landscapes in Alaska and Sweden. J. Ecol. 95, 802–817. https://doi.org/10.1111/j.1365-2745.2007.01259.x.

Shindell, D.T., Faluvegi, G., Koch, D.M., Schmidt, G.A., Unger, N., Bauer, S.E., 2009. Improved attribution of climate forcing to emissions. Science 326, 716–718. https://doi.org/10.1126/science.1174760.

Starr, G., Oberbauer, S.F., Ahlquist, L.E., 2008. The photosynthetic response of Alaskan tundra plants to increased season length and soil warming. Arct. Antarct. Alp. Res. 40, 181–191. https://doi.org/10.1657/1523-0430(06-015)[STARR]2.0.CO;2.

Stieglitz, M., Déry, S.J., Romanovsky, V.E., Osterkamp, T.E., 2003. The role of snow cover in the warming of arctic permafrost. Geophys. Res. Lett. 30, 1721. https://doi.org/10.1029/2003GL017337.

Stocker, T.F., Qin, D., Plattner, G.-K., Tignor, M.M.B., Allen, S.K., Boschung, J., Nauels, A., Xia, Y., Bex, V., Midgley, P.M., 2013. Long-term climate change: projections, commitments and irreversibility. In: Climate Change 2013: The Physical Science Basis (Contribution of Working Group I to the Fifth Assessment Report of the Intergovernmental Panel on Climate Change).

Street, L.E., Shaver, G.R., Williams, M., Van Wijk, M.T., 2007. What is the relationship between changes in canopy leaf area and changes in photosynthetic CO_2 flux in arctic ecosystems? J. Ecol. 95, 139–150. https://doi.org/10.1111/j.1365-2745.2006.01187.x.

Street, L.E., Subke, J.-A., Sommerkorn, M., Sloan, V., Ducrotoy, H., Phoenix, G.K., Williams, M., 2013. The role of mosses in carbon uptake and partitioning in arctic vegetation. New Phytol. 199, 163–175. https://doi.org/10.1111/nph.12285.

Stuefer, S.L., Kane, D.L., Dean, K.M., 2020. Snow water equivalent measurements in remote Arctic Alaska watersheds. Water Resour. Res. 56, e2019WR025621. https://doi.org/10.1029/2019WR025621.

Sturm, M., Schimel, J., Michaelson, G., Welker, J.M., Oberbauer, S.F., Liston, G.E., Fahnestock, J., Romanovsky, V.E., 2005. Winter biological processes could help convert Arctic Tundra to shrubland. BioScience 55, 17–26. https://doi.org/10.1641/0006-3568(2005)055[0017:WBPCHC]2.0.CO;2.

Subin, Z.M., Koven, C.D., Riley, W.J., Torn, M.S., Lawrence, D.M., Swenson, S.C., 2013. Effects of soil moisture on the responses of soil temperatures to climate change in cold regions*. J. Climate 26, 3139–3158. https://doi.org/10.1175/JCLI-D-12-00305.1.

Sweet, S.K., Griffin, K.L., Steltzer, H., Gough, L., Boelman, N.T., 2015. Greater deciduous shrub abundance extends tundra peak season and increases modeled net CO_2 uptake. Glob. Change Biol. 21, 2394–2409. https://doi.org/10.1111/gcb.12852.

Tape, K., Sturm, M., Racine, C., 2006. The evidence for shrub expansion in northern Alaska and the Pan-Arctic. Glob. Change Biol. 12, 686–702. https://doi.org/10.1111/j.1365-2486.2006.01128.x.

Tape, K.D., Hallinger, M., Welker, J.M., Ruess, R.W., 2012. Landscape heterogeneity of shrub expansion in Arctic Alaska. Ecosystems 15, 711–724. https://doi.org/10.1007/s10021-012-9540-4.

Treat, C.C., Virkkala, A.-M., Burke, E., Bruhwiler, L., Chatterjee, A., Fisher, J.B., Hashemi, J., Parmentier, F.-J.W., Rogers, B.M., Westermann, S., Watts, J.D., Blanc-Betes, E., Fuchs, M., Kruse, S., Malhotra, A., Miner, K., Strauss, J., Armstrong, A., Epstein, H.E., Gay, B., Goeckede, M., Kalhori, A., Kou, D., Miller, C.E., Natali, S.M., Oh, Y., Shakil, S., Sonnentag, O., Varner, R.K., Zolkos, S., Schuur, E.A.G., Hugelius, G., 2024. Permafrost carbon: progress on understanding stocks and fluxes across northern terrestrial ecosystems. J. Geophys. Res. Biogeosciences 129, e2023JG007638. https://doi.org/10.1029/2023JG007638.

Uhlířová, E., Šantrůčková, H., Davidov, S.P., 2007. Quality and potential biodegradability of soil organic matter preserved in permafrost of Siberian tussock tundra. Soil Biol. Biochem. 39, 1978–1989. https://doi.org/10.1016/j.soilbio.2007.02.018.

van Pelt, W.J.J., Kohler, J., Liston, G.E., Hagen, J.O., Luks, B., Reijmer, C.H., Pohjola, V.A., 2016. Multidecadal climate and seasonal snow conditions in Svalbard. Case Rep. Med. 121, 2100–2117. https://doi.org/10.1002/2016JF003999.

Vickers, D., Thomas, C.K., Martin, J.G., Law, B., 2009. Self-correlation between assimilation and respiration resulting from flux partitioning of eddy-covariance CO_2 fluxes. Agric. For. Meteorol. 149, 1552–1555. https://doi.org/10.1016/j.agrformet.2009.03.009.

Voigt, C., Lamprecht, R.E., Marushchak, M.E., Lind, S.E., Novakovskiy, A., Aurela, M., Martikainen, P.J., Biasi, C., 2016. Warming of subarctic tundra increases emissions of all three important greenhouse gases – carbon dioxide, methane, and nitrous oxide. Glob. Change Biol. https://doi.org/10.1111/gcb.13563 n/a-n/a.

Wahren, C.-H.A., Walker, M.D., Bret-Harte, M.S., 2005. Vegetation responses in Alaskan arctic tundra after 8 years of a summer warming and winter snow manipulation experiment. Glob. Change Biol. 11, 537–552. https://doi.org/10.1111/j.1365-2486.2005.00927.x.

Walker, M.D., 1996. Community baseline measurements for ITEX studies. ITEX Man. Eds MolauU MølgaardP Dan. Polar Cent. Cph. Den. 2, 39–41.

Walker, M.D., Walker, D.A., Auerbach, N.A., 1994. Plant communities of a tussock tundra landscape in the Brooks Range Foothills, Alaska. J. Veg. Sci. 5, 843–866. https://doi.org/10.2307/3236198.

Walker, M.D., Walker, D.A., Welker, J.M., Arft, A.M., Bardsley, T., Brooks, P.D., Fahnestock, J.T., Jones, M.H., Losleben, M., Parsons, A.N., et al., 1999. Long-term experimental manipulation of winter snow regime and summer temperature in arctic and alpine tundra. Hydrol. Process. 13, 2315–2330.

Walker, M.D., Wahren, C.H., Hollister, R.D., Henry, G.H.R., Ahlquist, L.E., Alatalo, J.M., Bret-Harte, M.S., Calef, M.P., Callaghan, T.V., Carroll, A.B., Epstein, H.E., Jónsdóttir, I.S., Klein, J.A., Magnússon, B., Molau, U., Oberbauer, S.F., Rewa, S.P., Robinson, C.H., Shaver, G.R., Suding, K.N., Thompson, C.C., Tolvanen, A., Totland, Ø., Turner, P.L., Tweedie, C.E., Webber, P.J., Wookey, P.A., 2006. Plant community responses to experimental warming across the tundra biome. Proc. Natl. Acad. Sci. 103, 1342–1346. https://doi.org/10.1073/pnas.0503198103.

Watts, J.D., Natali, S.M., Minions, C., Risk, D., Arndt, K., Zona, D., Euskirchen, E.S., Rocha, A.V., Sonnentag, O., Helbig, M., Kalhori, A., Oechel, W., Ikawa, H., Ueyama, M., Suzuki, R., Kobayashi, H., Celis, G., Schuur, E.A.G., Humphreys, E., Kim, Y., Lee, B.-Y., Goetz, S., Madani, N., Schiferl, L.D., Commane, R., Kimball, J.S., Liu, Z., Torn, M.S., Potter, S., Wang, J.A., Jorgenson, M.T., Xiao, J., Li, X., Edgar, C., 2021. Soil respiration strongly offsets carbon uptake in Alaska and Northwest Canada. Environ. Res. Lett. 16, 084051. https://doi.org/10.1088/1748-9326/ac1222.

Weg, M.J. van de, Shaver, G.R., Salmon, V.G., 2013. Contrasting effects of long term versus short-term nitrogen addition on photosynthesis and respiration in the Arctic. Plant Ecol. 214, 1273–1286. https://doi.org/10.1007/s11258-013-0250-6.

Welker, J.M., Fahnestock, J.T., Jones, M.H., 2000. Annual CO_2 flux in dry and moist Arctic Tundra: field responses to increases in summer temperatures and winter snow depth. Clim. Change 44, 139–150. https://doi.org/10.1023/A:1005555012742.

Williams, M., Street, L.E., Wijk, M.T. van, Shaver, G.R., 2006. Identifying differences in carbon exchange among Arctic ecosystem types. Ecosystems 9, 288–304. https://doi.org/10.1007/s10021-005-0146-y.

Wipf, S., Rixen, C., 2010. A review of snow manipulation experiments in Arctic and alpine tundra ecosystems. Polar Res. 29, 95–109. https://doi.org/10.1111/j.1751-8369.2010.00153.x.

Xue, K., Yuan, M., M., J., Shi, Z., Qin, Y., Deng, Y., Cheng, L., Wu, L., He, Z., Van Nostrand, J.D., Bracho, R., Natali, S., Schuur, E.A.G., Luo, C., Konstantinidis, K.T., Wang, Q., Cole, J.R., Tiedje, J.M., Luo, Y., Zhou, J., 2016. Tundra soil carbon is vulnerable to rapid microbial decomposition under climate warming. Nat. Clim. Change 6, 595–600. https://doi.org/10.1038/nclimate2940.

Zhang, T., 2005. Influence of the seasonal snow cover on the ground thermal regime: an overview. Rev. Geophys. 43, RG4002. https://doi.org/10.1029/2004RG000157.

Zhang, X., He, J., Zhang, J., Polyakov, I., Gerdes, R., Inoue, J., Wu, P., 2013. Enhanced poleward moisture transport and amplified northern high-latitude wetting trend. Nat. Clim. Chang. 3, 47–51. https://doi.org/10.1038/nclimate1631.

Zona, D., Lafleur, P.M., Hufkens, K., Bailey, B., Gioli, B., Burba, G., Goodrich, J.P., Liljedahl, A.K., Euskirchen, E.S., Watts, J.D., Farina, M., Kimball, J.S., Heimann, M., Göckede, M., Pallandt, M., Christensen, T.R., Mastepanov, M., López-Blanco, E., Jackowicz-Korczynski, M., Dolman, A.J., Marchesini, L.B., Commane, R., Wofsy, S.C., Miller, C.E., Lipson, D.A., Hashemi, J., Arndt, K.A., Kutzbach, L., Holl, D., Boike, J., Wille, C., Sachs, T., Kalhori, A., Song, X., Xu, X., Humphreys, E.R., Koven, C.D., Sonnentag, O., Meyer, G., Gosselin, G.H., Marsh, P., Oechel, W.C., 2022. Earlier snowmelt may lead to late season declines in plant productivity and carbon sequestration in Arctic tundra ecosystems. Sci. Rep. 12, 3986. https://doi.org/10.1038/s41598-022-07561-1.